Development of Methods for Structural Characterization of *Pantoea stewartii* Quorum-Sensing Regulator EsaR

Kayla K. Pennerman

Thesis submitted to the faculty of the Virginia Polytechnic Institute and State University in partial fulfillment of the requirements for the degree of

Master of Science
in
Biological Sciences

Ann M. Stevens, Committee Chair
David Bevan
David L. Popham
Florian D. Schubot

December 11, 2013

Blacksburg, VA

Keywords: EsaR, LuxR homologue, *Pantoea stewartii*, quorum sensing, FRET

Development of Methods for Structural Characterization of *Pantoea stewartii* Quorum-Sensing Regulator EsaR

Kayla Pennerman

Abstract

The LuxR family of proteins serves as quorum-sensing transcriptional regulators in proteobacteria. At high population densities, a small acyl-homoserine lactone (AHL) molecule, produced by a LuxI homologue, accumulates in the environment. The LuxR proteins bind to their respective AHL when the ligand accumulates to sufficient levels. Once bound to AHL, the holoproteins usually become functional as transcriptional activators. However, there is a subset of LuxR homologues, the EsaR subfamily, which is active without the AHL ligand and becomes inactivated once bound to it. EsaR is the best understood member of this subfamily. It controls virulence in the corn pathogen *Pantoea stewartii* ssp. *stewartii*.

Solubility issues have previously limited structural studies of LuxR homologues as the proteins could not be purified without the AHL ligand. A soluble recombinant EsaR protein, HMGE, is biologically active and can be purified in the absence and presence of AHL, unlike most other LuxR homologues. Using HMGE, amino acid substitutions and Förster resonance energy transfer **(**FRET**)**, experimental methods were designed for determining the dimerization interface of EsaR and for testing the hypothesis that EsaR undergoes a conformational shift when presented with the AHL ligand.

To identify residues of the dimerization interface, heterodimerization assays were designed, involving either coexpression or coincubation of wild-type EsaR and variant HMGE proteins. In this assay, the inability of the proteins to copurify by nickel affinity chromatography would indicate that the modified residue(s) are important for dimerization of EsaR. To determine

the conformational change that EsaR undergoes when bound to the AHL ligand, a FRET assay was developed to estimate the distances between amino acid residues in the absence and presence of AHL. Future work will have to include a few modifications to the methods and/or control experiments. This study provides the basis upon which the present methods can be further developed and later used for structural studies of EsaR.

Acknowledgements

To my advisor, Dr. Stevens, I didn't intend to, but I've given you some unnecessary stress. I'm sorry for that. Despite that, you still worked to get me over the finish line. My sincere thanks, I really needed it and am thankful for it.

To my committee members, thank you for your helpful comments and advice. I feel that I've grown some as a scientist by anticipating your questions. I want to especially acknowledge Dr. Schubot. You've been my unofficial co-advisor. I'm truly grateful for the time and energy you've spent on my research and me.

To my labmates, Revathy and Alison, it's been fun working and occasionally joking around with you two. Thanks for answering all my random questions. Revathy, congrats on your upcoming defense (you'll do great) and your future career. Alison, you're going to be the head grad student once Revathy graduates, but it's clear that you're ready for it.

To the other students, staff and faculty of the Life Sciences I building, I haven't met all of you. But, the interactions have always been positive and sometimes enlightening. The number one reason to work in LSI is the people you get to meet. The scenery is second.

To the members of the Molecular Plant Sciences group, I didn't stay as long as planned, but I enjoyed every second I spent with you all.

Last, but certainly not least, I want to thank my family and friends, whom I'm very lucky to have. You've provided me with so much advice and support. Without you, I wouldn't be the person I am today. And it's because of you that I have confidence in myself and my future. I can only hope that I've been able to give back a portion of what you've given me. Thank you.

Table of contents

Page number

List of figures

Page number

List of tables

Page number

Chapter one

Literature review

Introduction to quorum-sensing

Quorum-sensing (QS) is a phenomenon in which bacteria are able to communicate their population densities through small chemical signaling molecules. This type of cell-cell communication facilitates coordination of gene expression within a population. QS is found in eubacteria, especially proteobacteria, which use this ability to exhibit cooperative properties and actions such as bioluminescence, virulence and biofilm production [reviewed in (1, 2)]. Such QS-controlled behaviors have significant impacts on human health and agricultural yields. Rational inhibition or stimulation of QS for health or agricultural purposes requires a solid understanding of the structural and mechanistic aspects of these regulatory systems.

Bioluminescence as a result of QS in *Vibrio fischeri*

QS was first described in the marine proteobacterium *Vibrio fischeri* (formerly *Photobacterium fischeri*) in the 1970s (3, 4). This organism may be free-living or form symbiotic relationships with certain fish and squid. It inhabits the light organ of the Japanese pinecone fish, *Monocentris japonica*, at densities up to 10^{10} cells per milliliter (5). At such high cell densities, *V. fischeri* is luminescent as a result of luciferase activity, which is controlled via QS. The luciferase enzyme catalyzes the oxidation of a reduced flavin mononucleotide and the conversion of a long-chain aldehyde to a long-chain acid in the presence of oxygen gas, producing an unstable photon-emitting intermediate [reviewed in (6)].

Kempner and Hanson found that light intensity is not a simple direct function of bacterial growth (3). The addition of "conditioned" medium, in which *V. fischeri* cells were previously grown and then removed, resulted in a light intensity pattern that more closely followed the bacterial growth curve. In this case, the amount of light emitted from a culture increased as the

bacteria grew. It was argued that the medium contained an inhibitory "dialyzable factor". However, their efforts in isolating this inhibitor were unsuccessful (3).

Nealson *et al.* later discovered that bioluminescence in *V. fischeri* is an induced process requiring the production and accumulation of a small signaling molecule, known as "autoinducer" – referring to the fact that it is synthesized by the bacteria themselves (4). Experimental evidence pointed to regulation of bioluminescence at the level of transcription or translation as light production could be stopped with the use of inhibitors of either mRNA or protein synthesis (4).

Genes required for *V. fischeri* bioluminescence

Advancements in recombinant DNA technology allowed for the eventual characterization of the structural and regulatory elements required for light production in *V. fischeri*. Engebrecht *et al.* isolated a 9 kb fragment that caused transformed *Escherichia coli* cells to express luciferase and become luminescent at high cell densities (7). The genetic functions contained in the fragment were determined through transposon-generated mutations and complementation studies, leading to the conclusion that there were two divergently-transcribed units. One affects production of autoinducer, luciferase and aldehyde; the other, response to autoinducer. A subsequent study using similar techniques identified seven essential genes: *luxA-E* and *luxI* in the *lux* operon, and *luxR* in the other unit (8). The *luxA* and *luxB* genes encode the luciferase subunits, and *luxC, luxD, luxE* are involved in aldehyde production. The *luxI* and *luxR* genes regulate luciferase production.

LuxI/LuxR QS system in *V. fischeri*

The protein products of *luxI* and *luxR* are LuxI and LuxR, respectively (8). These are the primary regulators of the transcription of the *lux* genes together with a low molecular weight

signaling molecule, which is produced by LuxI, *N*-(3-oxo-hexanoyl)-L-homoserine lactone (Table 1.1), an acyl homoserine lactone (AHL) [reviewed in (1, 9)]. At low cell density, LuxI produces AHL at basal levels (10). This molecule freely diffuses across the cell membrane, allowing it to accumulate within the surrounding medium (1). As the population density increases, AHL levels increase. At high concentrations, AHL interacts with LuxR which is then able to function as a transcriptional activator of the *lux* operon (11-13). This effects a positive feedback loop in which more LuxI is generated, leading to more production of AHL, which binds to and activates more LuxR.

Homologous QS systems in other bacteria

There are several known types of bacterial QS systems using different signaling molecules including AHL, aryl homoserine lactones, peptides, furanosyl borate diesters, bradyoxetins, butyrolactones or fatty acid-derived compounds [reviewed in (1, 14-16)]. Over 100 AHL-based QS systems utilizing LuxI and LuxR homologues are found in other proteobacteria, some species even employing multiple AHL signals and LuxR homologues [reviewed in (1, 15, 16)]. Such systems are involved in cell division regulation in *E. coli*, conjugal transfer of Ti plasmids in *Agrobacterium tumefaciens*, nitrogen fixation in *Rhizobium leguminosarum* and virulence factor productions in *Pseudomonas aeruginosa* and *Pantoea stewartii* [reviewed in (1, 17)]. The cognate signal molecules are structurally similar and sometimes have limited cross-reactivity with other LuxR proteins, though unique structural aspects of LuxR-like proteins ultimately control ligand specificities (17-20).

P. stewartii pathogenesis in corn hosts

P. stewartii (formerly *Erwinia stewartii*) is a destructive phytopathogen that causes Stewart's wilt disease in susceptible *Zea mays* varieties and was first described in sweet corn in the state of New York (21). Its primary vector is *Chaetocnema pulicaria*, the corn flea beetle, which feeds on seedling leaves (22). After introduction to the host vascular system, the bacteria begin to proliferate within the apoplast. Growth in the intercellular spaces of leaves can result in a symptom known as "watersoaking", in which there is a visible accumulation of fluids outside of the host cell membranes (22-24).

At a higher population density within the xylem, the bacteria begin the production of stewartan exopolysaccharides (EPS) which help support their extension away from plant cell walls into the open middle of xylem vessels (25). The combination of a high number of bacterial cells and coordinated EPS production results in the clogging of the pit membranes in the xylem by formation of a biofilm. For laboratory-generated QS mutant populations in which stewartan production is constitutive or nonexistent, surface adhesion and extension is poor (22, 25, 26). The bacteria also move throughout the plant less efficiently, and disease-associated lesions may be limited. This indicates that temporal control of EPS production is required for disease progression (22, 25, 26).

QS regulation of stewartan production in *P. stewartii*

The virulence genes of *P. stewartii* were first organized into three complementation groups on the chromosomal DNA (27). The first and second groups harbored the *hrp*/*wts* genes that code for type III secretion systems and hypersensitive responses in non-hosts (28-31). The third group contained *rcsA*, a gene encoding for a co-activator of the *wce* (formerly *cps*) genes

involved in stewartan production (24, 32). Other required genes involved in pathogenicity were discovered at later dates (29, 33).

Regulation of stewartan production has two layers. There is direct regulation by the Rcs two-component signal transduction system (15, 24). In this system, perception of environmental signals results in phosphorylation and activation of RcsB, which forms a complex with RcsA to function as a transcriptional activator of the *rcsA*, *hrp* and *wce* genes. A LuxI/LuxR-type QS system holds stewartan production under a secondary but dominant control by repressing expression of *rcsA* (Fig. 1.1) (26, 34-37). EsaR binds between the two promoters of *rcsA*, one of which allows for basal expression, the other is up-regulated by the RcsAB transcription factor (37). The low amount of RcsA that is translated when apo-EsaR is active is mostly degraded by Lon protease and is not able to form many complexes with RcsB (15, 24, 35, 36).

EsaI/EsaR QS system in *P. stewartii*

QS in *P. stewartii* follows a similar mechanism as that in *V. fischeri*, but with some key differences. The LuxI and LuxR homologues EsaI and EsaR synthesize the signaling molecule and interact with it, respectively (26, 34). The AHL molecule produced by EsaI is identical to that used in *V. fischeri*. However, unlike LuxR, EsaR may behave as either a repressor or an activator of transcription depending on the position of its target DNA sequence relative to the start site of the regulated gene (35-39). It blocks RNA polymerase binding to the promoters of *rcsA* and *esaR*, yet appears to up-regulate expression of a putative sRNA gene (38). Derepression occurs at higher AHL concentrations when EsaR binds with AHL, decreasing its ability to bind DNA. This interaction stabilizes EsaR *in vitro*, as indicated by the increase in the apparent melting temperature of the holoprotein (35). Results from the Stevens Lab (Virginia Tech) have

now demonstrated that EsaR is directly involved in the repression and activation of several additional genes (40).

LuxR structure and function

The LuxR protein has two functional domains: a carboxyl-terminal domain (CTD) and an amino-terminal domain (NTD) (13, 41-43). Purified CTD binds *in vitro* to the *lux* box upstream of the *lux* operon in cooperation with RNA polymerase (11, 44). This portion of the protein has amino acid sequence similarity to other protein regions involved in DNA binding and contains a predicted helix-turn-helix (HTH) motif (41). The NTD is involved in AHL interaction; mutations in this domain render LuxR nonresponsive to the ligand molecule (13, 41).

LuxR protein family

LuxR homologues only have 18 to 25% overall amino acid identity; stronger similarities are found in the regions corresponding to the predicted HTH motif in the CTD and the AHL-binding site in the NTD [reviewed in (1, 17)]. Stevens *et al.* divide the LuxR family of proteins into five classes on the basis of their interactions with AHL (1). Class 1 regulators are irreversibly bound to AHL. The signaling molecule is incorporated into the stable structure of the protein during translation. Class 2 homologues also bind AHL cotranslationally but may dissociate from AHL. Classes 2 and 3 require AHL binding to stably dimerize and function though the latter may fold properly without AHL. Class 4 regulators, members of the EsaR subfamily, are inactivated upon AHL binding, distinguishing themselves from the previous classes in this regard. Class 4 regulators have predicted structures similar to other LuxR proteins save for an extended interdomain linker region and an extended CTD (1). Class 5 LuxR

homologues do not dimerize and are not known to interact with self-produced AHL, but rather with signaling molecules from other bacteria (1).

Inhibition of LuxR proteins for therapeutic purposes

Impeding AHL-mediated expression of bacterial virulence factor genes would be an attractive method of disease control as it would affect specific bacterial functions (45). However, because of the structural similarities among systems, control methods may still affect a range of pathogens (16). Targets include the LuxI/LuxR proteins and the AHL molecule, to interfere with AHL production, reception and accumulation. Many natural compounds produced by plants, animals and bacterial have been shown to prevent QS-regulated pathogenesis [reviewed in (16, 46, 47)]. These comprise extra- and intracellular acylases and lactonases which degrade AHL, and antagonistic furanone compounds which have lactone moieties and diminish the activity and stability of proteins involved in QS.

Rational inhibition of LuxR homologues in QS systems have primarily focused on the design of AHL analogs and non-analogous structures which bind competitively to the AHL-binding pocket of the NTD. AHL analogs can be varied in three main parts: the acyl chain, the central amide and the lactone moiety [reviewed in (1)]. After their design, the molecules can be tested via high-throughput screening and/or virtual screening. Many molecules have proven to be very effective, having IC_{50} values in the micromolar and nanomolar ranges (1, 45, 48, 49). However, explanations as to how these molecules work rely mostly on activity assays and molecular modeling to simulate the different conformations and interactions of active and inactive protein. Structural studies of LuxR proteins with and without their ligands may allow for better design and understanding of antagonists and agonists.

Structures of LuxR homologues

Structures have been determined for ligand-bound TraR, SdiA, LasR, CviR and QscR.

TraR

TraR, found in *A. tumefaciens*, is involved in the regulation of conjugal transfer of the Ti plasmid between bacteria (18). Its structure was solved in two nearly identical asymmetric complexes with its cognate AHL and target DNA sequence (the *tra* box) (50, 51). The asymmetry of the protein dimer is due to the different conformations of the linker region. It is slightly more elongated in one monomer than in the other. This also results in polar NTD-CTD contacts within one monomer, but not the other.

The DNA-binding CTD consists of four α-helices, two of which form a helix-turn-helix (HTH) motif (50). The recognition helix is supported by hydrophobic interactions with the scaffolding helix and a salt-bridge between the recognition helix and a second CTD helix. Each TraR monomer makes five direct contacts with the target DNA, binding to one of two halves of the *tra* box. Four contacts are made by the recognition helix, one by its salt-bridged partner. The other two helices may provide extra interactions.

The NTD is composed of five antiparallel β-sheets surrounded by three α-helices on either side (50). TraR requires AHL for stability (1, 51, 52). The ligand is completely embedded within the active site between the β-sheets and three of the α-helices (50). This molecule is secured within the cavity by hydrophobic interactions and two separate hydrogen bonds with the nitrogen atom and the carbonyl oxygen in the lactone moiety. The NTD-NTD dimerization interface involves hydrophobic interactions between two corresponding nearly parallel helices

and a turn between two β-sheets. It covers more surface area than the CTD-CTD dimerization interface.

SdiA

SdiA is a monomeric Class 5 LuxR homologue regulator found in enteric bacteria such as *E. coli* (1). It is not known to have a cognate signal molecule, but will interact with AHLs from other organisms. Like TraR, it appears to require a ligand to fold (53). The NTD structure of SdiA was calculated with NMR data from solubilized purified protein bound to a non-cognate AHL (*N*-octanoyl-L-homoserine lactone). The structure is remarkably similar to the NTD of TraR, having a configuration of antiparallel β-sheets with surrounding helices. The signaling molecule is again buried in a hydrophobic pocket, between the five β-sheets, two of the five α-helices and the two 3_{10} helices. This cavity is larger than that of TraR, which may allow for better accommodation of different AHLs (1, 53).

LasR

The crystal structure of the NTD of LasR from *P. aeruginosa* in complex with AHL has been solved (19). This structure also has an α-β-α sandwich arrangement comparable to that found in the NTD of TraR. The hydrogen-bonding network of the solvent-accessible AHL is, however, more extensive than of buried AHL in TraR. There are six hydrogen bonds, one of which is water-mediated. The NTD-NTD dimerization interface of LasR involves helices which are perpendicular to one another rather than parallel.

CviR

The crystal structure of full-length CviR from *Chromobacterium violaceum* was solved bound to a strongly antagonistic chlorolactone compound and as several NTD-AHL complexes (20). The separate domains of CviR are similar to those of TraR, containing an HTH motif in the CTD and an α-β-α sandwich configuration in the NTD. The root-mean-square deviations (rmsd) between corresponding domains of different proteins are small (2.4 Å for the NTDs and 1.9 Å for the CTDs) (20). Bound to an antagonist, CviR exhibits a crossed-domain dimer structure in which the NTD and the CTD of different monomers are in close contact. The CTDs of this "closed conformation" are ~60 Å apart instead of ~30 Å as in active TraR, an unfavorable spread for DNA binding.

QscR

QscR is another LuxR homologue found in *P. aeruginosa*. It strongly interacts with the AHL synthesized by LasI (54). Its full-length dimerized structure was determined by X-ray crystallography in complex with AHL (55). The CTD contains an HTH motif, and the NTD comprises an α-β-α sandwich which binds the signaling molecule by hydrogen bonds and hydrophobic interactions. The stabilization of the AHL ligand is similar to that seen in LasR. The rmsds for the separate corresponding TraR and QscR domains are low (1.61 Å for the NTDs and 1.50 Å for the CTDs), and they can be closely aligned to one another (Fig. 1.2) (55). However, rather than a dimer formed of parallel subunits, QscR monomers actually intersect. As a result, the dimerization interface of QscR is much more extensive. The NTD of one monomer interacts with both domains of the other monomer.

Limitations of LuxR structural studies

As of yet, LuxR homologue structures have only been solved in complex with AHL or its analogs. For most of these proteins, the AHL ligand is required for stable folds and is buried within the structure (56). Lack of solubility has also been a restriction of some studies (16). These limitations do not allow for the study of most apoprotein structures. As such, the conformational changes that occur in response to cognate ligand binding have not been observed.

Research objectives and justifications

This work aimed to continue structural studies of EsaR. Methods were designed to tackle two objectives: identification of the amino acid residues which are important for dimerization of EsaR and determination of the conformations of EsaR in the absence and presence of the AHL ligand. It has been hypothesized that, when bound to AHL, EsaR undergoes a conformational shift in which the CTDs spread further apart from one another, inhibiting binding to the target DNA sequence (20). This hypothesis was visualized with homology models of EsaR built using the structures of active QscR and inactive CviR (Fig. 1.3).

EsaR appears to undergo conformational shifts when interacting with AHL (39). Upon binding to AHL, the protein is protected in certain regions from limited hydrolysis by protease and also has a slightly different elution peak during size-exclusion chromatography. EsaR is relatively more stably folded than most other LuxR proteins and can be isolated with or without AHL (39). This property makes EsaR a potential model protein for studying LuxR conformational changes in response to ligand binding because both purified apoprotein and holoprotein are obtainable for *in vitro* analyses. Results from such studies may be generalizable to other LuxR-like proteins, especially those in the EsaR subfamily.

A hexahistidine (His6) and maltose binding protein (MBP) fused EsaR (HMGE) is soluble, biologically active and can be purified in the absence and presence of AHL (39). Using amino acid variations (Chapter Two) and Förster resonance energy transfer **(**FRET**)** analysis (Chapter Three) of HMGE, methods to investigate the conformational structures of EsaR were designed.

References

1. Stevens AM, Queneau Y, Soulere L, von Bodman S, Doutheau A. 2011. Mechanisms and synthetic modulators of AHL-dependent gene regulation. *Chem Rev* 111:4-27.
2. Stevens AM, Schuster M, Rumbaugh KP. 2012. Working together for the common good: cell-cell communication in bacteria. *J Bacteriol* 194:2131-41.
3. Kempner ES, Hanson FE. 1968. Aspects of light production by *Photobacterium fischeri*. *J Bacteriol* 95:975-9.
4. Nealson KH, Platt T, Hastings JW. 1970. Cellular control of the synthesis and activity of the bacterial luminescent system. *J Bacteriol* 104:313-22.
5. Ruby EG, Nealson KH. 1976. Symbiotic association of *Photobacterium fischeri* with the marine luminous fish *Monocentris japonica*; a model of symbiosis based on bacterial studies. *Biol Bull* 151:574-86.
6. Nealson KH, Hastings JW. 1979. Bacterial bioluminescence: its control and ecological significance. *Microbiol Rev* 43:496-518.
7. Engebrecht J, Nealson K, Silverman M. 1983. Bacterial bioluminescence: isolation and genetic analysis of functions from *Vibrio fischeri*. *Cell* 32:773-81.
8. Engebrecht J, Silverman M. 1984. Identification of genes and gene products necessary for bacterial bioluminescence. *Proc Natl Acad Sci U S A* 81:4154-8.
9. Schaefer AL, Val DL, Hanzelka BL, Cronan JE, Greenberg EP. 1996. Generation of cell-to-cell signals in quorum sensing: acyl homoserine lactone synthase activity of a purified *Vibrio fischeri* LuxI protein. *Proc Natl Acad Sci U S A* 93:9505-9.
10. Kaplan HB, Greenberg EP. 1985. Diffusion of autoinducer is involved in regulation of the *Vibrio fischeri* luminescence system. *J Bacteriol* 163:1210-4.
11. Stevens AM, Greenberg EP. 1997. Quorum sensing in *Vibrio fischeri*: essential elements for activation of the luminescence genes. *J Bacteriol* 179:557-62.
12. Urbanowski ML, Lostroh CP, Greenberg EP. 2004. Reversible acyl-homoserine lactone binding to purified *Vibrio fischeri* LuxR protein. *J Bacteriol* 186:631-7.
13. Shadel GS, Young R, Baldwin TO. 1990. Use of regulated cell lysis in a lethal genetic selection in *Escherichia coli*: identification of the autoinducer-binding region of the LuxR protein from *Vibrio fischeri* ATCC7744. *J Bacteriol* 172:3980-7.
14. Sturme MH, Kleerebezem M, Nakayama J, Akkermans AD, Vaugha EE, de Vos WM. 2002. Cell to cell communication by autoinducing peptides in Gram-positive bacteria. *Antonie Van Leeuwenhoek* 81:233-43.
15. von Bodman SB, Bauer WD, Coplin DL. 2003. Quorum sensing in plant-pathogenic bacteria. *Annu Rev Phytopathol* 41:455-82.
16. Churchill ME, Chen L. 2011. Structural basis of acyl-homoserine lactone-dependent signaling. *Chem Rev* 111:68-85.
17. Fuqua WC, Winans SC, Greenberg EP. 1994. Quorum sensing in bacteria: the LuxR-LuxI family of cell density-responsive transcriptional regulators. *J Bacteriol* 176:269-75.
18. Piper KR, Beck von Bodman S, Farrand SK. 1993. Conjugation factor of *Agrobacterium tumefaciens* regulates Ti plasmid transfer by autoinduction. *Nature* 362:448-50.
19. Bottomley MJ, Muraglia E, Bazzo R, Carfi A. 2007. Molecular insights into quorum sensing in the human pathogen *Pseudomonas aeruginosa* from the structure of the virulence regulator LasR bound to its autoinducer. *J Biol Chem* 282:13592-600.
20. Chen G, Swem LR, Swem DL, Stauff DL, O'Loughlin CT, Jeffrey PD, Bassler BL, Hughson FM. 2011. A strategy for antagonizing quorum sensing. *Mol Cell* 42:199-209.

21. Stewart FC. 1897. A bacterial disease of sweet corn. *N.Y. Agric. Exp. Stat.* 130:422-439.
22. Braun EJ. 1982. Ultrastructural investigation of resistant and susceptible maize inbreds infected with *Erwinia stewartii*. *Cytology and Histology* 72:159-166.
23. Bradshaw-Rouse JJ, Whatley MH, Coplin DL, Woods A, Sequeira L, Kelman A. 1981. Agglutination of *Erwinia stewartii* strains with a corn agglutinin: correlation with extracellular polysaccharide production and pathogenicity. *Appl Environ Microbiol* 42:344-50.
24. Torres-Cabassa A, Gottesman S, Frederick RD, Dolph PJ, Coplin DL. 1987. Control of extracellular polysaccharide synthesis in *Erwinia stewartii* and *Escherichia coli* K-12: a common regulatory function. *J Bacteriol* 169:4525-31.
25. Koutsoudis MD, Tsaltas D, Minogue TD, von Bodman SB. 2006. Quorum-sensing regulation governs bacterial adhesion, biofilm development, and host colonization in *Pantoea stewartii* subspecies *stewartii*. *Proc Natl Acad Sci U S A* 103:5983-8.
26. von Bodman SB, Majerczak DR, Coplin DL. 1998. A negative regulator mediates quorum-sensing control of exopolysaccharide production in *Pantoea stewartii* subsp. *stewartii*. *Proc Natl Acad Sci U S A* 95:7687-92.
27. Coplin DL, Frederick RD, Majerczak DR, Haas ES. 1986. Molecular cloning of virulence genes from *Erwinia stewartii*. *J Bacteriol* 168:619-23.
28. Coplin DL, Frederick, RD, Majerczak, DR, Tuttle, LD. 1992. Characterization of a gene cluster that specifies pathogenicity in *Erwinia stewartii*. *Mol Plant Microbe Interact* 5:81-88.
29. Coplin DL, Frederick, RD, Majerczak, DR. 1992. New pathogenicity loci in *Erwinia stewartii* identified by random Tn5 mutagenesis and molecular cloning. *Mol Plant Microbe Interact* 5:266-268.
30. Frederick RD, Ahmad M, Majerczak DR, Arroyo-Rodriguez AS, Manulis S, Coplin DL. 2001. Genetic organization of the *Pantoea stewartii* subsp. *stewartii hrp* gene cluster and sequence analysis of the *hrpA*, *hrpC*, *hrpN*, and *wtsE* operons. *Mol Plant Microbe Interact* 14:1213-22.
31. Merighi M, Majerczak DR, Stover EH, Coplin DL. 2003. The HrpX/HrpY two-component system activates *hrpS* expression, the first step in the regulatory cascade controlling the Hrp regulon in *Pantoea stewartii* subsp. *stewartii*. *Mol Plant Microbe Interact* 16:238-48.
32. Dolph PJ, Majerczak DR, Coplin DL. 1988. Characterization of a gene cluster for exopolysaccharide biosynthesis and virulence in *Erwinia stewartii*. *J Bacteriol* 170:865-71.
33. Carlier A, Burbank L, von Bodman SB. 2009. Identification and characterization of three novel EsaI/EsaR quorum-sensing controlled stewartan exopolysaccharide biosynthetic genes in *Pantoea stewartii* ssp. *stewartii*. *Mol Microbiol* 74:903-13.
34. Beck von Bodman S, Farrand SK. 1995. Capsular polysaccharide biosynthesis and pathogenicity in *Erwinia stewartii* require induction by an N-acylhomoserine lactone autoinducer. *J Bacteriol* 177:5000-8.
35. Minogue TD, Wehland-von Trebra M, Bernhard F, von Bodman SB. 2002. The autoregulatory role of EsaR, a quorum-sensing regulator in *Pantoea stewartii* ssp. *stewartii*: evidence for a repressor function. *Mol Microbiol* 44:1625-35.

36. Minogue TD, Carlier AL, Koutsoudis MD, von Bodman SB. 2005. The cell density-dependent expression of stewartan exopolysaccharide in *Pantoea stewartii* ssp. *stewartii* is a function of EsaR-mediated repression of the *rcsA* gene. *Mol Microbiol* 56:189-203.
37. Carlier AL, von Bodman SB. 2006. The *rcsA* promoter of *Pantoea stewartii* subsp. *stewartii* features a low-level constitutive promoter and an EsaR quorum-sensing-regulated promoter. *J Bacteriol* 188:4581-4.
38. Schu DJ, Carlier AL, Jamison KP, von Bodman S, Stevens AM. 2009. Structure/function analysis of the *Pantoea stewartii* quorum-sensing regulator EsaR as an activator of transcription. *J Bacteriol* 191:7402-9.
39. Schu DJ, Ramachandran R, Geissinger JS, Stevens AM. 2011. Probing the impact of ligand binding on the acyl-homoserine lactone-hindered transcription factor EsaR of *Pantoea stewartii* subsp. *stewartii*. *J Bacteriol* 193:6315-22.
40. Ramachandran R, Stevens AM. 2013. Proteomic analysis of the quorum-sensing regulon in *Pantoea stewartii* and identification of direct targets of EsaR. *Appl Environ Microbiol* 79:6244-52.
41. Slock J, vanRiet D, Kolibachuk D, Greenberg EP. 1990. Critical regions of the *Vibrio fischeri* LuxR protein defined by mutational analysis. *J Bacteriol* 172:3974-9.
42. Choi SH, Greenberg EP. 1991. The C-terminal region of the *Vibrio fischer*i LuxR protein contains an inducer-independent *lux* gene activating domain. *Proc Natl Acad Sci U S A* 88:11115-9.
43. Choi SH, Greenberg EP. 1992. Genetic dissection of DNA binding and luminescence gene activation by the *Vibrio fischeri* LuxR protein. *J Bacteriol* 174:4064-9.
44. Stevens AM, Dolan KM, Greenberg EP. 1994. Synergistic binding of the *Vibrio fischeri* LuxR transcriptional activator domain and RNA polymerase to the *lux* promoter region. *Proc Natl Acad Sci U S A* 91:12619-23.
45. Koch B, Liljefors T, Persson T, Nielsen J, Kjelleberg S, Givskov M. 2005. The LuxR receptor: the sites of interaction with quorum-sensing signals and inhibitors. *Microbiology* 151:3589-602.
46. Zhang LH. 2003. Quorum quenching and proactive host defense. *Trends Plant Sci* 8:238-44.
47. Lazar V. 2011. Quorum sensing in biofilms--how to destroy the bacterial citadels or their cohesion/power?. *Anaerobe* 17:280-5.
48. Sabbah M, Soulere L, Reverchon S, Queneau Y, Doutheau A. 2011. LuxR dependent quorum sensing inhibition by N,N'-disubstituted imidazolium salts. *Bioorg Med Chem* 19:4868-75.
49. Boukraa M, Sabbah M, Soulere L, El Efrit ML, Queneau Y, Doutheau A. 2011. AHL-dependent quorum sensing inhibition: synthesis and biological evaluation of alpha-(N-alkyl-carboxamide)-gamma-butyrolactones and alpha-(N-alkyl-sulfonamide)-gamma-butyrolactones. *Bioorg Med Chem Lett* 21:6876-9.
50. Vannini A, Volpari C, Gargioli C, Muraglia E, Cortese R, De Francesco R, Neddermann P, Di Marco S. 2002. The crystal structure of the quorum sensing protein TraR bound to its autoinducer and target DNA. *EMBO J* 21:4393-401.
51. Vannini A, Volpari C, Gargioli C, Muraglia E, De Francesco R, Neddermann P, Di Marco S. 2002. Crystallization and preliminary X-ray diffraction studies of the transcriptional regulator TraR bound to its cofactor and to a specific DNA sequence. *Acta Crystallogr D Biol Crystallogr* 58:1362-4.

52. Pinto UM, Winans SC. 2009. Dimerization of the quorum-sensing transcription factor TraR enhances resistance to cytoplasmic proteolysis. *Mol Microbiol* 73:32-42.
53. Yao Y, Martinez-Yamout MA, Dickerson TJ, Brogan AP, Wright PE, Dyson HJ. 2006. Structure of the *Escherichia coli* quorum sensing protein SdiA: activation of the folding switch by acyl homoserine lactones. *J Mol Biol* 355:262-73.
54. Oinuma K, Greenberg EP. 2011. Acyl-homoserine lactone binding to and stability of the orphan *Pseudomonas aeruginosa* quorum-sensing signal receptor QscR. *J Bacteriol* 193:421-8.
55. Lintz MJ, Oinuma K, Wysoczynski CL, Greenberg EP, Churchill ME. 2011. Crystal structure of QscR, a *Pseudomonas aeruginosa* quorum sensing signal receptor. *Proc Natl Acad Sci U S A* 108:15763-8.
56. Zhu J, Winans SC. 2001. The quorum-sensing transcriptional regulator TraR requires its cognate signaling ligand for protein folding, protease resistance, and dimerization. *Proc Natl Acad Sci U S A* 98:1507-12.
57. Holm L, Kaariainen S, Rosenstrom P, Schenkel A. 2008. Searching protein structure databases with DaliLite v.3. *Bioinformatics* 24:2780-1.
58. Schwede T, Kopp J, Guex N, Peitsch MC. 2003. SWISS-MODEL: An automated protein homology-modeling server. *Nucleic Acids Res* 31:3381-5.

Tables and figures

Table 1.1. Cognate AHL ligands of some LuxR proteins.

Molecule Name	Structure	LuxR receptor(s)
N-(3-oxo-hexanoyl)-L-homoserine lactone	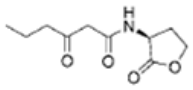	LuxR and EsaR
N-(3-oxo-octanoyl)-L-homoserine lactone	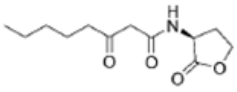	TraR
N-hexanoyl-L-homoserine lactone	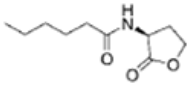	CviR
N-(3-oxo-octanoyl)-L-homoserine lactone	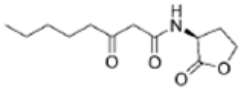	LasR and QscR

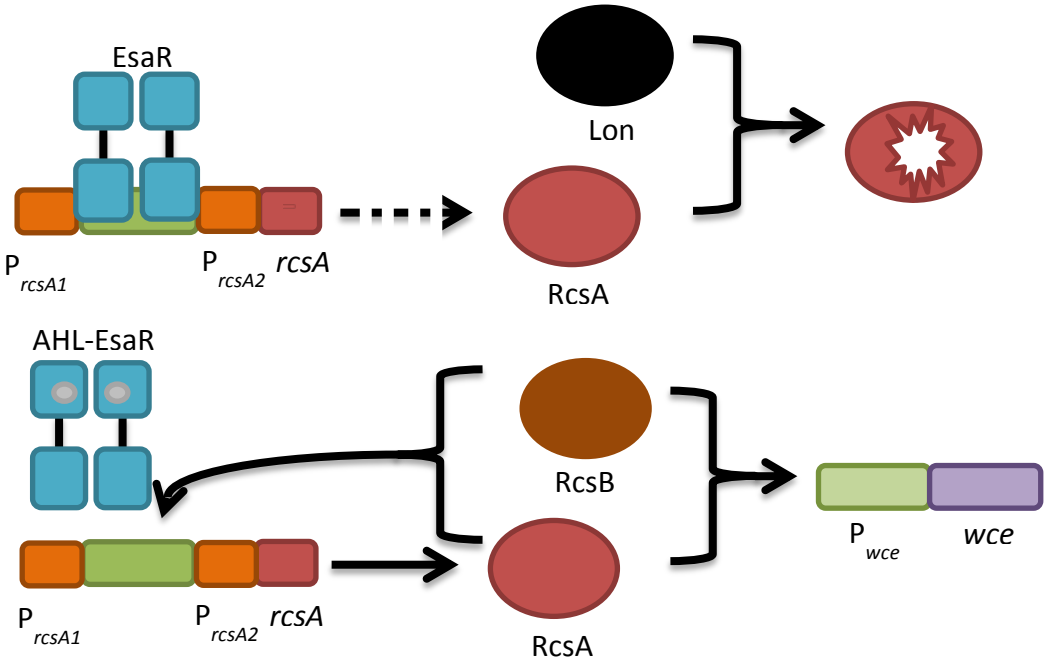

Figure 1.1. Regulation of *rcsA* in *P. stewartii* by EsaR. (A) At low cell densities, EsaR blocks transcription of *rcsA*. A low amount of RcsA is made and is destroyed by Lon protease. (B) At high cell densities, AHL inactivates EsaR, allowing for a higher transcription rate of *rcsA*. The protease is not able to degrade all of the RcsA, the remainder of which stably dimerizes with RcsB to up-regulate transcription of certain genes.

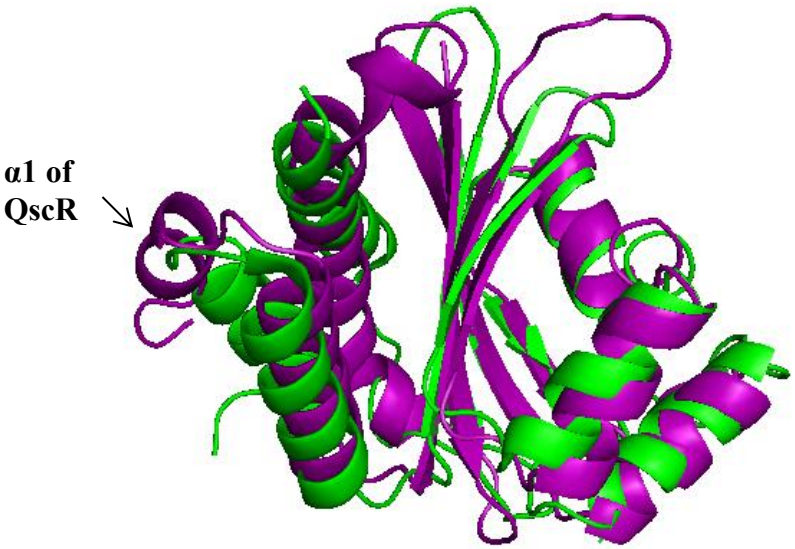

Figure 1.2. Alignment of TraR (green) and QscR (purple) NTDs. α1 of QscR is indicated. The alignment was constructed with DaliLite (57). The image was rendered using the PyMOL Molecular Graphics System, Version 1.3 Schrödinger, LLC.

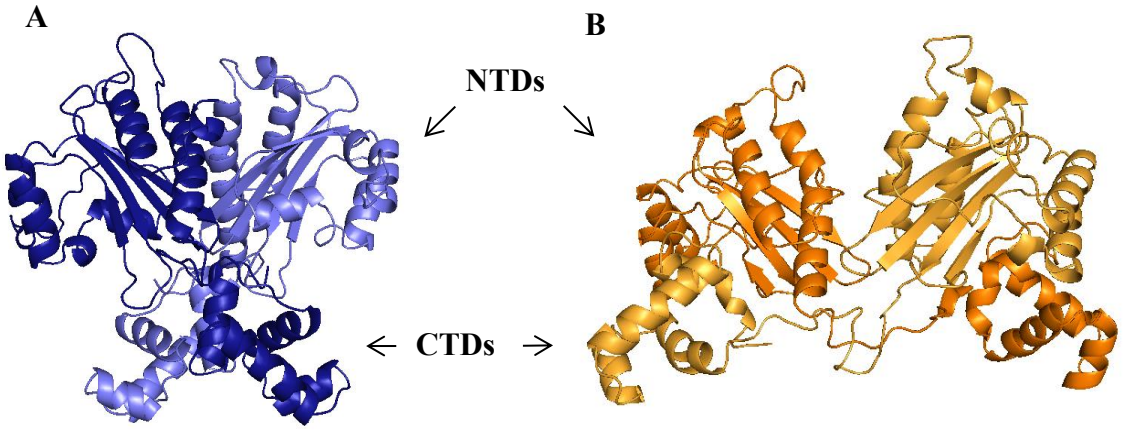

Figure 1.3. Homology models of EsaR. Models were based on (A) active QscR associated with its cognate AHL ligand and (B) inactive CviR bound to an artificial antagonist (PDB codes 3SZT and 3QP5, respectively (20, 55)). The CTDs are spread further apart in the CviR-based model. Monomers are differently colored. Images rendered using the PyMOL Molecular Graphics System, Version 1.3 Schrödinger, LLC and SWISS-MODEL (58).

Chapter two

Methods to study the dimerization interface of EsaR

Abstract

The quorum-sensing regulator EsaR from the phytopathogen *Pantoea stewartii* is thought to function as a homodimer, activating and repressing transcription of select genes in the absence of its ligand. In this study, two heterodimerization assays were designed to characterize EsaR residues for their respective roles in dimerization. These assays involved either *in vivo* coexpression or *in vitro* coincubation of wild-type and variant EsaR proteins. Copurification of wild-type and variant EsaR by nickel affinity chromatography was indicative of the formation of heterodimers between the two proteins. It was expected that the variant proteins that were not able to dimerize would not be able to copurify with wild-type EsaR.

These assays were tested using 17 single amino acid variants of His-MBP tagged EsaR (HMGE). The residues were selected based on homology models to QscR from *Pseudomonas aeruginosa* and CviR from *Chromobacterium violaceum*. Site-directed mutagenesis was used to generate the desired amino acid substitutions. The variant proteins were examined for stability via western immunoblotting and then characterized for their ability to oligomerize with wild-type EsaR. The results demonstrate that more control experiments and/or adjustments to the buffer conditions or the purification strategy are needed to discourage the wild-type protein from sticking to the nickel affinity column and to prevent possible proteolysis of HMGE. However, copurification of wild-type and variant EsaR is possible, indicating oligomerization.

Introduction

Many proteobacteria use quorum-sensing (QS) to communicate their population densities via the production and perception of a membrane-diffusible acyl-homoserine lactone (AHL) signaling molecule. This type of cell-cell communication permits bacteria to exhibit cooperative

properties and actions such as bioluminescence, virulence and biofilm production (1, 2). LuxR proteins are the master protein regulators of these QS systems. They are usually dimeric proteins that interact with the signaling molecule and directly affect gene transcription (1). Most LuxR homologues are active when bound to their cognate AHL molecule. EsaR, a LuxR homologue found in the corn pathogen *Pantoea stewartii*, and other members of its subfamily behave in an opposite manner and are inactivated by binding to AHL.

Despite its different response to AHL binding, EsaR is predicted to share structural features with other LuxR-like proteins; the N-terminal domain binds the AHL ligand and the C-terminal domain binds the target DNA sequence (1). As the EsaR protein can be purified in the absence of AHL, unlike most LuxR homologues, it is an attractive subject for structure/function studies. LuxR homologues usually function as dimers, therefore, knowledge of the dimerization interface would help with efforts to disrupt or enhance the functions of these proteins. To identify residues of EsaR involved in dimerization, *in vivo* and *in vitro* assays were designed to test for the relative importance of residues for dimerization.

Materials and methods

Bacterial strains, plasmids and growth conditions

Escherichia coli Top10 was used in all experiments (3). Bacteria were grown at 37°C in Luria broth (LB) medium (w/v 1% Bacto-tryptone, 0.5% Bacto-yeast extract and 0.5% NaCl). Liquid medium was aerated by shaking at 250 rpm in an incubator (New Brunswick Scientific Innova 4200). Solid LB medium used for plating transformants contained an additional w/v 1.5% Bacto-agar. Bacteria were transformed with mutant plasmids following an established protocol (4). Antibiotic and reagent supplements included ampicillin (100 μg/ml), chloramphenicol (20

μg/ml), isopropyl-β-D-1-thiogalactopyranoside (IPTG; 1 mM), L-arabinose (0.02%) and 5-bromo-4-chloro-3-indolyl-β-D-galactopyranoside (20 μg/ml) as appropriate. Information on utilized plasmids and bacterial strains can be found in Table 2.1.

For protein overexpression, cells sampled from a freezer stock (v/v 17% glycerol; kept at -70°C) were grown overnight in 5 ml of liquid LB medium containing the appropriate antibiotic(s) to maintain the plasmid(s). Subcultures were made to an optical density at 600 nm (OD_{600}) of 0.05 (measurements made using a Spectronic 20+, Thermo Spectronic). Once the subcultures reached mid-log stage of growth (used cultures were at OD_{600} ranging from 0.5 to 0.7), protein overexpression was induced with IPTG to a final concentration of 1 mM and/or L-arabinose to a final concentration of 0.02%. For a single titration experiment, IPTG was added to final concentrations of 0, 0.1, 0.25, 0.5, 0.75 and 1 mM. Cultures were left shaking at 250 rpm overnight at 19°C (depending on the amount of culture and sizes of flasks, either an E24 or an E25 New Brunswick Scientific Excella incubator was used). The following day, the cultures were removed from the incubator and placed in ice for at least 20 min, and cells were harvested by centrifugation in a Beckman Coulter JA-10 or JA-25.50 rotor (7,000 xg for 10 min at 4°C). Cell pellets were frozen at -70°C for later use.

Prediction of amino acid residues involved in dimerization of EsaR

Initial amino acids of interest were selected based on an EsaR homology model constructed by M. Churchill's group (University of Colorado). The model fit the amino acid sequence of EsaR against the corresponding residues in the known structure of QscR (5). Based on this model, thirteen residues were predicted to be located on the dimerization interface of the N-terminal domain of EsaR: V36, S37, K38, K39, N40, V69, I70, L71, T72, R76, D116, H117

and N119. Another three residues, D52, L45 and H115, were among those identified by additional modeling. Different EsaR models were constructed using the known structures of QscR and CviR, and the online homology model builder SWISS-MODEL (5-7) (Fig. 1.3). PDBsum was used to identify residues potentially involved in dimerization (8). Residues D52, R76, D116, H115, H117 and N119 were predicted to be involved in interactions between the two N-terminal domains. The other residues were predicted to be involved in interactions between the N-terminal and C-terminal domains of different monomers.

Site-directed mutagenesis of pHMGE plasmids

Unless otherwise stated, site-directed mutagenesis was used to generate variants of EsaR tagged at the N-terminus with hexahistidine residues (His) and maltose binding protein (MBP) (HMGE, wild-type or variant) via the QuikChange Lighting Site-Directed Mutagenesis kit (Agilent Technologies). The pHMGE plasmid served as a template for oligonucleotide primers (Integrated DNA Technologies) containing the desired mutations (Tables 2.1 and 2.2). The instructions for the QuikChange kit were followed with two exceptions during the transformation step: *E. coli* Top10 cells were used instead of the provided *E. coli* XL-10 strain, and LB medium was used instead of the suggested NZY+ broth.

To generate HMGE variants D52F, R76E and H117F, mutagenesis was conducted in a PCR-like fashion with the Phusion enzyme (New England Biolabs). Reaction compositions and thermocycling conditions followed the manufacturer's protocol for using Phusion with the following exceptions. Eighteen cycles were permitted with an annealing temperature of 55°C. In the situation that a reaction failed, this temperature was increased up to 3°C below the melting temperature of the primer set and/or the extension time was increased by a minute. After site-

directed mutagenesis, 1 µl of DpnI was added to 20 µl of the reaction product. The mixture was then incubated at 37°C for one hour. This depleted the methylated template before transforming the mutant plasmid into *E. coli* Top10.

Each mutation was confirmed by Sanger sequencing of isolated plasmids (performed by the Virginia Bioinformatics Institute, Core Facility). Plasmids were purified using the QIAprep Spin Miniprep Kit (Qiagen). For each sequencing reaction, the Virginia Bioinformatics Institute was given 10 µl of purified plasmid at 100 ng/µl and 5 µl of primer at 5 µM. Primers used for sequencing are specified in Table 2.2. These were used to determine the nucleotide sequences of the *tac* promoter region, the His-MBP tag and glycine linker. In addition, mutation primers N40AF, V69AR and L71AR were used to sequence *esaR*.

Variant protein stabilities were assayed by a western immunoblot of cell lysates containing overexpressed variant HMGE proteins induced with 1 mM IPTG. Whole cell lysates were prepared for sodium dodecyl sulfate polyacrylamide gel electrophoresis (SDS-PAGE) by resuspending harvested cells to an OD_{600} = 20 and boiling as described below. On a 16-lane 12% SDS-PAGE gel, 5 µl was loaded into each well. Primary anti-EsaR antibodies courtesy of S. B. von Bodman (University of Connecticut/National Science Foundation) were used. The antibodies were diluted 1:500 in NET buffer (150 mM NaCl, 5 mM EDTA, 54.6 mM Tris-HCl, 8 mM Tris-base, v/v 0.05% Triton X-100, w/v 0.25% gelatin). Western immunoblots were conducted as described by Schu *et al.* (9).

Heterodimerization assay – coexpression method

The methods developed for the heterodimerization assays were based off the work conducted by U. Pinto and S. Winans (10). The first involved *in vivo* co-expression of HMGE or

variant HMGE with wild-type EsaR (wtEsaR). In this method, 5 ml of culture (LB medium containing 100 µg/ml ampicillin and 20 µg/ml chloramphenicol) with cells harboring plasmids encoding HMGE or variant HMGE (pHMGE), and wtEsaR (pSUP102-*esaR*) in the mid-log stage of growth (OD_{600} = 0.5 – 0.7) were induced to overexpress wtEsaR from pSUP102-*esaR* with 0.02% arabinose. Variant or non-variant HMGE was produced due to leaky expression of pHMGE under the P_{tac} promoter. The cultures were left shaking at 250 rpm, 19°C overnight. The following morning, cells were harvested by centrifugation (7,000 xg for 10 min, 4°C in an Eppendorf microcentrifuge 5417R) and frozen at -70°C for later use. Enough cells were collected so resuspension in 5 ml of buffer would result in an OD_{600} = 5. Cells containing HMGE variant R76E were grown in 50 ml of LB medium; enough cells were collected so resuspension in 5 ml of buffer would result in an OD_{600} = 25.

Frozen cells harboring HMGE or variant HMGE, and wtEsaR were thawed on ice and resuspended to an OD_{600} = 5 in 5 ml of Ni binding buffer (500 mM NaCl, 20 mM HEPES, 20 mM imidazole, 10% glycerol, pH 7.4). Cells containing HMGE variant R76E were resuspended to an OD_{600} = 25 in 5 ml of Ni binding buffer. Cells were lysed by sonication (settings: amplification 20%, 10 s pulse on, 10 s pulse off, repeated 10 times; performed with a Fisher Scientific Model 500 Dismembrator attached to a double step 3.2 mm diameter microtip in a Branson Sonifier Sound Enclosure). Cell debris and aggregates were removed via centrifugation (at 10,600 xg for 20 min at 4°C in an Eppendorf microcentrifuge 5417R). Lysate was passed through a 0.45 µm pore size syringe filter (mixed cellulose ester membrane, Fisher Scientific) and manually applied to a chilled (around 4°C on ice or in a refrigerator) 1 ml HisTrap HP column (GE Healthcare) by syringe. Speed of liquid exiting the column was manually maintained at around 1.5 ml/min. After washing the column with 3 ml of cold Ni binding buffer,

2.5 ml of cold Ni elution buffer (500 mM NaCl, 20 mM HEPES, 300 mM imidazole, 10% glycerol, pH 7.4) was applied. The first 0.5 ml of the elution was discarded. The latter 2 ml was collected as one fraction. Columns were cleaned after each use by stripping and recharging as directed by the manufacturer.

From the 2 ml elution fraction, 0.5 ml was mixed with 0.5 ml of 10% trichloroacetic acid and incubated overnight at 4°C. The following day, precipitates were pelleted by centrifugation (20,000 xg for 15 min at 4°C in an Eppendorf microcentrifuge 5417R). The pellet was washed with 100% cold acetone, centrifuged again in the same manner, and air-dried at 37°C. Resuspension of the dried pellets in 20 µl of 0.05 M NaOH resulted in an 80X concentration of the elution fraction. In preparation for SDS-PAGE, 5X sample buffer (v/v 12.48% 1 M Tris pH 6.8, w/v 4% SDS, v/v 20.8% glycerol, v/v 10% β-mercaptoethanol, v/v 5% saturated bromophenol blue solution in water) was added to a final 1X concentration, and the sample was boiled for 10 min. On a 12% SDS-PAGE gel with 16 wells total, 5 µl of sample was loaded into each well. Following electrophoresis (90 V for 2 h), a western immunoblot was conducted using anti-EsaR antibodies at a 1:500 dilution (9).

Heterodimerization assay – coincubation method

In the second approach to the heterodimerization assay, one or two liters of cells in LB medium with 100 µg/ml ampicillin containing non-mutant or mutant pHMGE were induced with 1 mM IPTG to enhance production of the encoded protein overnight at 19°C. One liter of culture was grown for variants with intracellular accumulations similar to non-variant HMGE. Cultures with lower apparent variant intracellular HMGE concentrations were grown in two 1 L cultures. Cells were harvested by centrifugation (7,000 xg for 10 min at 4°C) and frozen at -70°C.

After thawing, cells were resuspended in at most 10 ml of Ni binding buffer and lysed by sonication using a Fisher Scientific Model 500 Dismembrator and the settings previously describe in the above section. Cell debris and aggregates were removed from the lysates by centrifugation and filtration as described in the section above. The cleared lysates were degassed by vacuum pressure and separately applied to a 5 ml HisTrap HP column (GE Healthcare) using fast-performance liquid chromatography at 4°C (performed with ÄKTApurifier, GE Healthcare) at a maximum rate of 5 ml/min. After washing the column with at least 100 ml of Ni binding buffer, bound protein was eluted with a 25 ml linear gradient of increasing amounts of Ni elution buffer.

Elution fractions containing the protein of interest (determined by 12% SDS-PAGE analysis) were pooled and concentrated to below 7 ml before performing size-exclusion chromatography in a HiPrep 26/60 Sephacryl S-200 HR column (GE Healthcare) equilibrated with HMGE working buffer (500 mM NaCl, 20 mM HEPES, 10% glycerol, pH 7.4). The maximum flow rate was 1 ml/min. Eluted HMGE proteins were collected and concentrated to at least 2 µM in an Amicon stirred cell. Concentrated proteins were stored at 4°C until use.

Cells harboring pSUP102-*esaR* were grown in 1 L of LB medium with 20 µg/ml chloramphenicol to an OD_{600} = 0.5 before inducing production of wtEsaR with 0.02% arabinose. The culture was left overnight at 19°C. The following day, cells were harvested by centrifugation in 15 ml conical tubes (7,000 xg for 10 min at 4°C) and stored at -70°C. Each tube contained enough cells so that resuspension in 7 ml would yield an OD_{600} = 7.

Cell lysate containing wtEsaR was obtained by thawing these cells on ice and resuspending them in 7 ml of Ni binding buffer. Cells were lysed by sonication as described in the above section. Purified HMGE or HMGE variant was added to 900 µl of cell lysate to a 250

nM concentration. Total volumes were brought to 1 ml by adding Ni binding buffer. Initial concentrations of the HMGE proteins were measured at 280 nm using a NanoPhotometer P-Class (IMPLEN). The extinction coefficient for HMGE proteins at this wavelength was calculated to be 1.412 g l^{-1} cm^{-1} or 100730 M^{-1} cm^{-1} using the online ExPASy ProtParam tool (11). None of the variations introduced tyrosine, tryptophan or cysteine residues, so variants were assumed to have the same extinction coefficient. After incubating the samples at room temperature for two hours, as done by Pinto and Winans, the pull-down assay was conducted as previously stated in the coexpression heterodimerization method (10).

Protein purification for circular dichroism spectroscopy

Proteins were purified first by nickel affinity chromatography as described above using an ÄKTApurifier, then by heparin affinity using a GE Healthcare 5 ml HiTrap Heparin HP column (heparin binding buffer: 10 mM $NaHPO_4$, 250 mM NaCl, 10% glycerol, pH 7.2; heparin elution buffer: 10 mM $NaHPO_4$, 800 mM NaCl, 10% glycerol, pH 7.2; maximum flow rate 5 ml/min at 4°C). At least 100 ml of heparin binding buffer was used to wash the column before proceeding with a 25 ml elution gradient. Concentrated elutant (1 ml) had its buffer exchanged to HMGE working buffer in a 5 ml GE Healthcare HiTrap Desalting column. Samples were then concentrated to 0.19 mg/ml, as indicated by absorbance at 280 nm, using Amicon Ultra 0.5 ml centrifugal filters.

Circular dichroism spectroscopy

Circular dichroism (CD) spectroscopy experiments were performed with a Jasco J-815 CD spectrometer at 20°C. For each sample, five measurements were taken and averaged every

0.5 nm from 260 nm to 185 nm. A bandwidth of 1.00 nm was used. Mean residue ellipticities were calculated using the corrected measurement at a given wavelength divided by the pathlength in millimeters, the molar concentration of protein and the number of residues per protein (12). Experiments were duplicated, and the results were averaged.

Results and discussion

Control experiments for coexpression heterodimerization assay

In order to test the efficacy of the coexpression heterodimerization assay, the assay was tested prior to characterizing 12 amino acid residues for their involvement in dimer formation of EsaR. It was designed so that after nickel affinity purification of coexpressed proteins, detection of the wild-type EsaR protein (wtEsaR) by a western immunoblot indicated that a particular variation did not hinder dimerization (Fig. 2.1, panel A). Controls were performed to ensure that detected wtEsaR required the HMGE protein to be purified by nickel affinity chromatography and that the detected wild-type protein was not, instead, degraded or fragmented HMGE (Fig. 2.2, lanes B2 and B3). When both proteins were coexpressed, the heterodimerization assay resulted in detection of EsaR proteins that were about 72 kD and 26 kD in size (Fig. 2.2, lane B1). These sizes corresponded to the expected sizes of HMGE and wtEsaR, ~73 kD and ~28 kD respectively, indicating that the two proteins oligomerized. Purification of HMGE using its His tag led to co-purification of wtEsaR that interacted with HMGE.

In the absence of HMGE, wtEsaR was not detected (Fig. 2.2, lane B2). The wild-type protein lacked a His tag to allow purification by nickel affinity by itself. No proteins were present inside the cell lysate that could be co-purified with wtEsaR. When HMGE was tested alone, one protein band around 72 kD was detected (Fig. 2.2, lane B3). This showed that the

previously detected 26 kD protein was not degraded HMGE, but wtEsaR which had been co-purified with HMGE.

During the coexpression assay, variant protein expression under the P_{tac} promoter was not induced. It was found that the HMGE protein was produced without added IPTG (Fig. 2.3, lane 0 mM). The resulting intracellular concentration of HMGE was enough to permit co-purification with wtEsaR. Parameters for manual nickel affinity purification were tested using coexpressed non-variant HMGE and wtEsaR (Fig. 2.4).

Analysis of alanine-substitution HMGE variants via coexpression heterodimerization assay

Mutant pHMGE plasmids encoding HMGE variants V36A, S37A, K38A, K39A, N40A, V69A, I70A, L71A, T72A, R76A, D116A, H117A and N119A were generated by site-directed mutagenesis and transformed into *E. coli* Top10. Variant and wild-type protein stabilities were evaluated by western immunoblotting after induction of overexpression with 1 mM IPTG (Fig. 2.5). HMGE variants K39A and D116A visibly differed from non-variant HMGE. K39A migrated faster, indicating a lower molecular weight. D116A accumulated to a lower intracellular concentration than the control and other variants. Efforts to reconstruct the mutations for these two variants did not yield different results. It is suspected that the alanine variation at those two positions affected the overall structure of the HMGE protein. K39A was excluded from further analysis via the heterodimerization assay.

The mutant plasmids were cotransformed with pSUP102-*esaR* into *E. coli* Top10. HMGE and wtEsaR expression was first checked by western immunoblotting (Fig. 2.6). The alanine variants were then subjected to the coexpression heterodimerization assay method. The results from this method did not indicate that any of the variants had a noticeable effect on the ability of

HMGE to oligomerize with wtEsaR. Following nickel affinity purification, wtEsaR was still detectable by a western immunoblot (Fig. 2.7).

Analysis of additional HMGE variants via coexpression heterodimerization assay

A positive result, in which wtEsaR was not detected in the elutant, was needed to determine the usefulness of the coexpression heterodimerization assay. Without a positive result, it could not be concluded if the assay could identify HMGE variants that were not able to dimerize or if wtEsaR would always be retained on the column and subsequently eluted as long as there was a HMGE protein present. In continued efforts to obtain a positive result, more potentially disruptive, non-alanine variants were generated: D52F, R76E and H115F. The mutant plasmids encoding these HMGE variants were co-transformed with pSUP102-*esaR* into *E. coli* Top10. Western immunoblotting indicated that D52F and H115F did not accumulate to detectable levels within cells under conditions where expression of non-variant HMGE was detectable (Fig. 2.8). This was likely the result of structural changes caused by the variations as the P_{tac} promoter controlling expression had the correct sequence (data not shown). R76E could be detected; however, it was produced at levels noticeably lower than the HMGE control despite induction with 1 mM IPTG.

The R76E variant was tested using the coexpression heterodimerization assay (Fig. 2.9). To account for the lower apparent accumulation of the variant, more cells were collected and used as mentioned in the Materials and methods section. It appeared that a positive result was obtained, and the R76E variant was unable to dimerize with wild-type EsaR protein. Compared to the positive control, HMGE, the amount of wtEsaR that complexed with R76E was undetectable. Circular dichroism spectroscopy was employed to check if the R76E variant had

secondary structure (Fig. 2.10). By this method, R76E seemed to have a secondary structure similar to the non-variant HMGE protein. The apparent loss of the ability of the variant to oligomerize with wtEsaR was likely not the result of incorrect folding. However, because the variant was less abundant than non-variant HMGE, this could have impacted its ability to form dimers. To determine if protein concentration was impacting the experiment, a coincubation assay was developed.

Control experiment for coincubation heterodimerization assay

A coincubation heterodimerization assay was used to equalize the amounts of variant and non-variant HMGE protein present in the assay (Fig. 2.1, panel B). Control titration experiments were performed to determine, at which non-variant HMGE concentrations, wtEsaR could be co-purified (Fig. 2.11). The control in which wtEsaR was in the absence of HMGE did not work optimally as wtEsaR was detectable at low levels after nickel affinity purification (Fig. 2.11, panels B and D, lane 6). It should not have been present in the elutant without HMGE. Since the intensity of the corresponding wtEsaR band on the western immunoblot was noticeably below that of detected wtEsaR from other samples which did include HMGE, that small amount of protein in the control sample was considered as background binding of wtEsaR to the column.

Analysis of HMGE variants via coincubation heterodimerization assay

Four other HMGE variants, L45R, L71R, H115R and H117R, were generated and tested along with R76E (Fig. 2.12). The results did not show any noticeable differences among the ability of the variants to be co-purified with wtEsaR (Fig. 2.13). However, controls included in the experiment indicated that clear conclusions could not be drawn. The wild-type protein was

detectable at low levels when there was not any HMGE protein to allow co-purification, and even when wtEsaR was not included in a sample (Fig. 2.13, lanes 2 and 8). TCA precipitated samples of the wash steps did not show any protein exiting the column right before the elution steps (data not shown).This suggested that wtEsaR was able to remain in the HisTrap column despite washing, and stripping and recharging the column. It is also possible the 2 h incubation at room temperature encouraged higher proteolytic activity. This could result in the detected 26 kD EsaR protein actually being partially degraded HMGE. However, the control with only wtEsaR did not have any HMGE that could be degraded (Fig. 2.13, lane 9).

Another control for this experiment would have been to add HMGE to *E. coli* Top10 lysate that did not contain wtEsaR. The results from this assay are thus uninterpretable as it is not certain whether the variant proteins co-purified with wtEsaR, or if wtEsaR was able to bind to the column by itself. Further optimization of the controls will be necessary before the coincubation assay may be reliably used.

Conclusions

Two heterodimerization assays were developed for the purpose of characterizing EsaR residues for their importance in dimerization. They were both tested with a few control experiments and several single amino acid residue variants of HMGE. The results from these trial tests indicated that the coexpression heterodimerization assay was more reliable. The controls for this assay produced the expected results. A different result was also obtained with one variant, R76E, in that wtEsaR was not detected in the elutant. This was encouraging because it demonstrated that wtEsaR did not simply appear in the elutant for all of the experiments. The coincubation heterodimerization assay was used in an attempt to verify the R76E result as one

that indicated an inability of a variant to dimerize. However, the controls for the latter assay indicated that detection of a wtEsaR band was not a clear indication of dimerization.

Further development of these assays may require several actions. Primarily, a positive result, in which there is an indication that an HMGE variant is unable to oligomerize with wtEsaR is still needed. If the current results from the coexpression assay are true, then they suggest that all the tested alanine variants were capable of dimerization. That would mean that EsaR has a relatively strong dimerization interface. In order to disturb it, more disruptive and/or multiple variations may be needed. Such variants may be unstable or otherwise unable to accumulate in a cell, as D52F and H115F were. It is not known if EsaR can remain folded as a monomer. If a variation completely disrupts dimerization of EsaR, the monomeric variant may not be testable.

Cross-linking could be considered as a method for testing different residues without attempting to disrupt the dimerization as done by Palzer *et al.* (13). Selected residues would be varied to one not present in non-variant HMGE, such as p-azido-L-phenylalanine (AzF). AzF is a photo-cross-linking amino acid that covalently links to nearby molecules when induced by UV light. After co-purification by nickel affinity, mass spectrometry would be used to identify proteins attached to HMGE and the residue(s) by which they attached. This work could also potentially give some insight to the folding of EsaR as amino acid residues which are proximal to each other would be more frequently cross-linked to the same AzF varied residue(s).

The consistent negative results could also indicate that the homology models for EsaR were inaccurate—the targeted residues may not be involved in dimerization. In this case, the assays should be evaluated by testing other variations at different residues. It may also be that some fault lies with the assay or the equipment. Before conducting the coexpression assay, it was

shown that wtEsaR alone could not be purified by nickel affinity purification. However, the negative results in the coincubation assay could also be caused by the HisTrap columns losing selectivity in the time that passed since those controls were performed or by the Ni binding buffer not having enough imidazole to discourage nonspecific binding to the column. Without a positive result (an observed deficiency in dimerization), it was impossible to tell if the methods worked as intended. If they did not, it would be best to modify and retest the assays before employing them.

Depending on the potential problems with the assay itself, protease inhibitors could be used to inhibit degradation of HMGE to a 26kD protein that could be mistaken for wtEsaR. A different tag could also be added to wtEsaR, such as glutathione S-transferase. Instead of using antibodies to detect both wtEsaR and HMGE, different antibodies would detect the different tags. The two proteins could not be confused with each other in this case.

Acknowledgments

Thanks are owed to several people. Mari Lehtimaki, Owen Richard and Mike Hughes generated the pHMGE mutants V36A, S37A, K38A, K39A, N40A, R76A, D116A, H117A and N119A. Susanne von Bodman gave us the anti-EsaR antibodies. Mair Churchill provided predictions using homology models based on QscR before the structure was published. Funding for this work was supplied by grant MCB-0919984 from the National Science Foundation and travel funds were received through a Lewis Edward Goyette Graduate Fellowship.

References

1. Stevens AM, Queneau Y, Soulere L, von Bodman S, Doutheau A. 2011. Mechanisms and synthetic modulators of AHL-dependent gene regulation. *Chem Rev* 111:4-27.
2. Stevens AM, Schuster M, Rumbaugh KP. 2012. Working together for the common good: cell-cell communication in bacteria. *J Bacteriol* 194:2131-41.
3. Grant SG, Jessee J, Bloom FR, Hanahan D. 1990. Differential plasmid rescue from transgenic mouse DNAs into *Escherichia coli* methylation-restriction mutants. *Proc Natl Acad Sci U S A* 87:4645-9.
4. Morrison DA. 1977. Transformation in *Escherichia coli*: cryogenic preservation of competent cells. *J Bacteriol* 132:349-51.
5. Lintz MJ, Oinuma K, Wysoczynski CL, Greenberg EP, Churchill ME. 2011. Crystal structure of QscR, a *Pseudomonas aeruginosa* quorum sensing signal receptor. *Proc Natl Acad Sci U S A* 108:15763-8.
6. Schwede T, Kopp J, Guex N, Peitsch MC. 2003. SWISS-MODEL: An automated protein homology-modeling server. *Nucleic Acids Res* 31:3381-5.
7. Chen G, Swem LR, Swem DL, Stauff DL, O'Loughlin CT, Jeffrey PD, Bassler BL, Hughson FM. 2011. A strategy for antagonizing quorum sensing. *Mol Cell* 42:199-209.
8. Laskowski RA. 2009. PDBsum new things. *Nucleic Acids Res* 37:7.
9. Schu DJ, Carlier AL, Jamison KP, von Bodman S, Stevens AM. 2009. Structure/function analysis of the *Pantoea stewartii* quorum-sensing regulator EsaR as an activator of transcription. *J Bacteriol* 191:7402-9.
10. Pinto UM, Winans SC. 2009. Dimerization of the quorum-sensing transcription factor TraR enhances resistance to cytoplasmic proteolysis. *Mol Microbiol* 73:32-42.
11. Greenfield NJ. 2006. Using circular dichroism spectra to estimate protein secondary structure. *Nature protocols* 1:2876-90.
12. Palzer S, Bantel Y, Kazenwadel F, Berg M, Rupp S, Sohn K. 2013. An expanded genetic code in *Candida albicans* to study protein-protein interactions *in vivo*. *Eukaryot Cell* 12:816-27.
13. Schu DJ, Ramachandran R, Geissinger JS, Stevens AM. 2011. Probing the impact of ligand binding on the acyl-homoserine lactone-hindered transcription factor EsaR of *Pantoea stewartii* subsp. *stewartii*. *J Bacteriol* 193:6315-22.
14. Riggs P. 2000. Expression and purification of recombinant proteins by fusion to maltose-binding protein. *Mol Biotechnol* 15:51-63.
15. Nallamsetty S, Austin BP, Penrose KJ, Waugh DS. 2005. Gateway vectors for the production of combinatorially-tagged His6-MBP fusion proteins in the cytoplasm and periplasm of *Escherichia coli*. *Protein Sci* 14:2964-71.
16. Simon R, O'Connell M, Labes M, Puhler A. 1986. Plasmid vectors for the genetic analysis and manipulation of rhizobia and other Gram-negative bacteria. *Methods Enzymol* 118:640-59.
17. Zhang RG, Pappas KM, Brace JL, Miller PC, Oulmassov T, Molyneaux JM, Anderson JC, Bashkin JK, Winans SC, Joachimiak A. 2002. Structure of a bacterial quorum-sensing transcription factor complexed with pheromone and DNA. *Nature* 417:971-4.

Tables and figures

Table 2.1. Plasmids and strains used in this study.

Plasmid/Strain	Relevant Information	Reference(s)
pHMGE	*attb*-His_6-MBP-TEV-Gly_5- *esaR-attb* under P_{tac}, Amp^r, derived from pDEST-HisMBP	(14)
pSUP102-*esaR*	*esaR* under $P_{BAD,}$ Cm^r	(9)
pMAL-P2	Backbone of pDEST-periHisMBP, *malE* under P_{tac}, Amp^r	(15, 16)
pSUP102	Compatible with pMAL-P2vectors, Cm^r	(17)
***E. coli* Top10**	Commercially available from Life Technologies	(18)
pV36A	Mutant pHMGE encoding variant V36A HMGE	This study
pS37A	Mutant pHMGE encoding variant S37A HMGE	This study
pK38A	Mutant pHMGE encoding variant K38A HMGE	This study
pK39A	Mutant pHMGE encoding variant K39A HMGE	This study
pN40A	Mutant pHMGE encoding variant N40A HMGE	This study
pL45R	Mutant pHMGE encoding variant L45R HMGE	This study
pD52F	Mutant pHMGE encoding variant D52F HMGE	This study
pV69A	Mutant pHMGE encoding variant V69A HMGE	This study
pI70A	Mutant pHMGE encoding variant I70A HMGE	This study
pL71A	Mutant pHMGE encoding variant L71A HMGE	This study
pL71R	Mutant pHMGE encoding variant L71R HMGE	This study
pT72A	Mutant pHMGE encoding variant T72A HMGE	This study
pR76A	Mutant pHMGE encoding variant R76A HMGE	This study
pR76E	Mutant pHMGE encoding variant R76E HMGE	This study
pH115R	Mutant pHMGE encoding variant D116A HMGE	This study
pD116A	Mutant pHMGE encoding variant H115R HMGE	This study
pH117A	Mutant pHMGE encoding variant H117A HMGE	This study
pH117F	Mutant pHMGE encoding variant H117F HMGE	This study
pH117R	Mutant pHMGE encoding variant H117R HMGE	This study
pN119A	Mutant pHMGE encoding variant N119A HMGE	This study

Table 2.2. Primers used in this study.

Primer[a]	Sequence[b]	T_m (°C)
	Site-directed mutagenesis primers	
V36AF	CGGATTACGCTTACACTGTTGCGAGCAAAAAAAATCCTTCAAAT	64.7
V36AR	ATTTGAAGGATTTTTTTTGCTCGCAACAGTGTAAGCGTAATCCG	64.7
S37AF	CGGATTACGCTTACACTGTTGTGGCCAAAAAAAATCCTTCAAATGTTC	65.4
S37AR	GAACATTTGAAGGATTTTTTTTGGCCACAACAGTGTAAGCGTAATCCG	65.4
K38AF	GGATTACGCTTACACTGTTGTGAGCGCAAAAAATCCTTCAAATGTTCT GATT	66.2
K38AR	AATCAGAACATTTGAAGGATTTTTTGCGCTCACAACAGTGTAAGCGTA ATCC	66.2
K38DF	GATTACGCTTACACTGTTGTGAGCGATAAAAATCCTTCAAATGTTCTG ATT	64.3
K38DR	AATCAGAACATTTGAAGGATTTTTATCGCTCACAACAGTGTAAGCGTA ATC	64.3
K39AF	GATTACGCTTACACTGTTGTGAGCAAAGCAAATCCTTCAAATGTTCTG ATTATTTC	65.1
K39AR	GAAATAATCAGAACATTTGAAGGATTTGCTTTGCTCACAACAGTGTAA GCGTAATC	65.1
N40AF	GATTACGCTTACACTGTTGTGAGCAAAAAAGCTCCTTCAAATGTTCTG ATTAT	65.1
N40AR	ATAATCAGAACATTTGAAGGAGCTTTTTTGCTCACAACAGTGTAAGCG TAATC	65.1
L45RF	CAAAAAAAATCCTTCAAATGTTCGGATTATTTCCAGTTATCCTGACG	62.5
L45RR	CGTCAGGATAACTGGAAATAATCCGAACATTTGAAGGATTTTTTTTG	62.5
D52FF	CCAGTTATCCTTTCGAATGGATTAGGTTATACCG	59.5
D52FR	CGGTATAACCTAATCCATTCGAAAGGATAACTGG	59.5
V69AF	GCTGACCGATCCGGCTATTCTCACGGCCT	67.9
V69AR	AGGCCGTGAGAATAGCCGGATCGGTCAGC	67.9
I70AF	TCAGCTGACCGATCCGGTTGCTCTCACGGCCTTTAAAC	68.9
I70AR	GTTTAAAGGCCGTGAGAGCAACCGGATCGGTCAGCTGA	68.9
L70RF	GTTTAAAGGCCGTGCGAATAACCGGATCGGTCAGC	66.9
L70RR	GCTGACCGATCCGGTTATTCGCACGGCCTTTAAAC	66.9
L71AF	CTTTCAGCTGACCGATCCGGTTATTGCCACGGCCTTTAAAC	67.7
L71AR	GTTTAAAGGCCGTGGCAATAACCGGATCGGTCAGCTGAAAG	67.7
T72AF	CCGATCCGGTTATTCTCGCGGCCTTTAAACGCA	67.1
T72AR	TGCGTTTAAAGGCCGCGAGAATAACCGGATCGG	67.1

R76AF	GGTTATTCTCACGGCCTTTAAAGCCACCTCGCCGTT	67.6
R76AR	AACGGCGAGGTGGCTTTAAAGGCCGTGAGAATAACC	67.6
R76EF	GGTTATTCTCACGGCCTTTAAAGAAACCTCGCCGTT	65.1
R76ER	AACGGCGAGGTTTCTTTAAAGGCCGTGAGAATAACC	65.1
H115FF	GGCTTTACCTATGTCCTGTTTGACCACATGAACAACC	63.9
H115FR	GGTTGTTCATGTGGTCAAACAGGACATAGGTAAAGCC	63.9
H115RF	CTTTACCTATGTCCTGCGTGACCACATGAACAACC	64.0
H115RR	GGTTGTTCATGTGGTCACGCAGGACATAGGTAAAG	64.0
D116AF	TACCTATGTCCTGCATGCCCACATGAACAACCTTG	65.2
D116AR	CAAGGTTGTTCATGTGGGCATGCAGGACATAGGTA	65.2
H117AF	TACCTATGTCCTGCATGACGCCATGAACAACCTTGCTCTG	67.3
H117AR	CAGAGCAAGGTTGTTCATGGCGTCATGCAGGACATAGGTA	67.3
H117FF	TACCTATGTCCTGCATGACTTTATGAACAACCTTGCTCTG	63.8
H117FR	CAGAGCAAGGTTGTTCATAAAGTCATGCAGGACATAGGTA	63.8
H117RF	CTATGTCCTGCATGACCGCATGAACAACCTTGCTC	65.7
H117RR	GAGCAAGGTTGTTCATGCGGTCATGCAGGACATAG	65.7
N119AF	GTCCTGCATGACCACATGGCCAACCTTGCTCTGTTGTC	68.7
N119AR	GACAACAGAGCAAGGTTGGCCATGTGGTCATGCAGGAC	68.7
	Sequencing primers	
tacF	TGACAATTAATCATCGGCTCGTATAATGT	56.4
tacHM_ rev	GGAACGCTTTGTCCGGGGTGATTTCAGC	65.1

[a] Site-directed mutagenesis primers were named with the original residue identity (using single letter code), position, resulting variation and forward (F) or reverse (R).

[b] Underlines indicate the altered codons for mutagenesis.

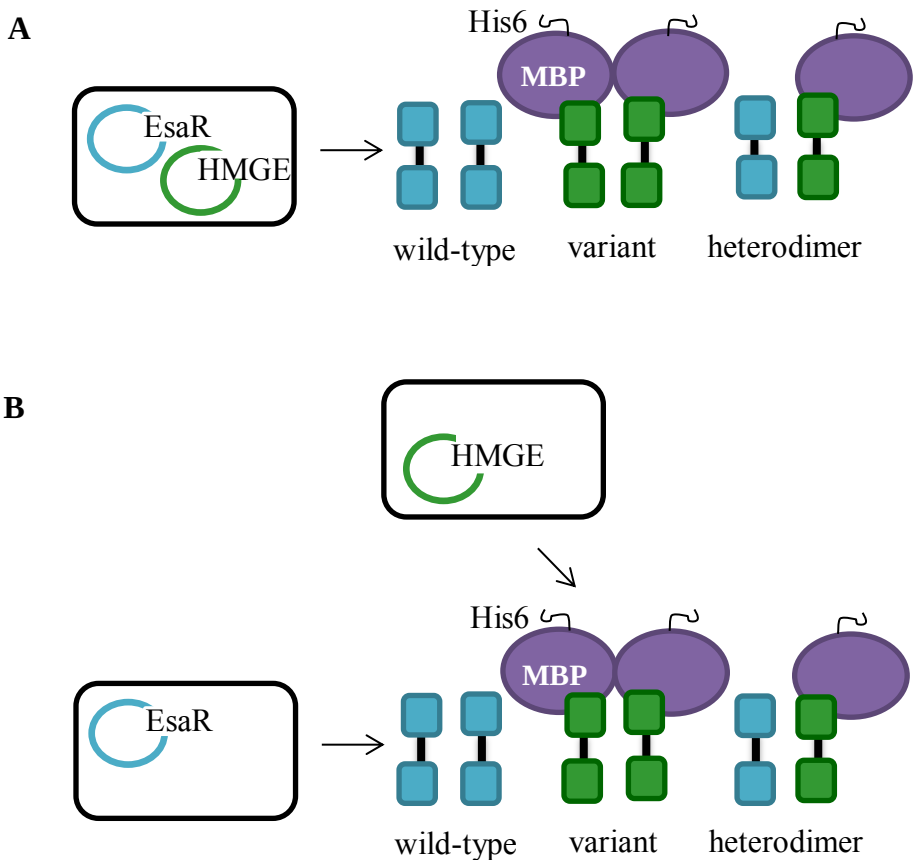

Figure 2.1. Cartoon model of heterodimerization assays. (A) Coexpressed or (B) coincubated proteins will form heterodimers if variant proteins were able to oligomerize with the wild-type protein. Wild-type protein can only be purified via nickel affinity chromatography when complexed with the variant.

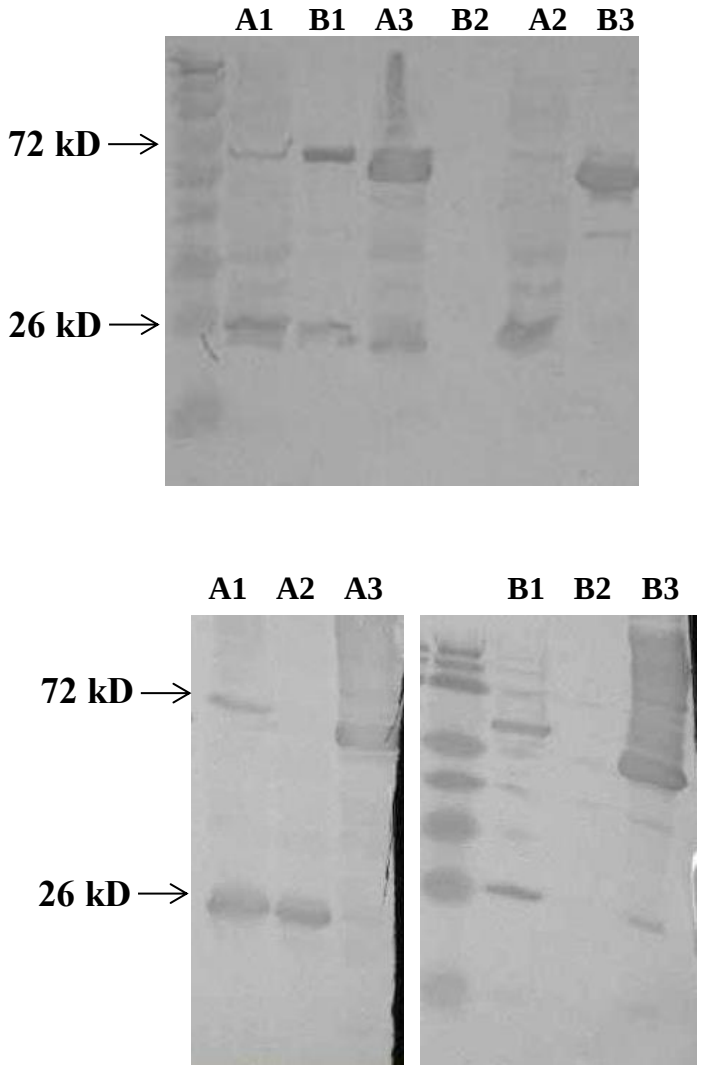

Figure 2.2. Controls for coexpression heterodimerization assay. Western immunoblots of (A) whole cell lysates and (B) proteins purified by nickel affinity are shown. Control strains containing cotransformed plasmids (1) pSUP102-*esaR* and pHMGE, (2) pSUP102-*esaR* and pMAL-P2, and (3) pSUP102 and pHMGE were used (Table 2.1). Detection of heterodimer formation was only possible when both wild-type and variant protein were present. Duplicated results are shown.

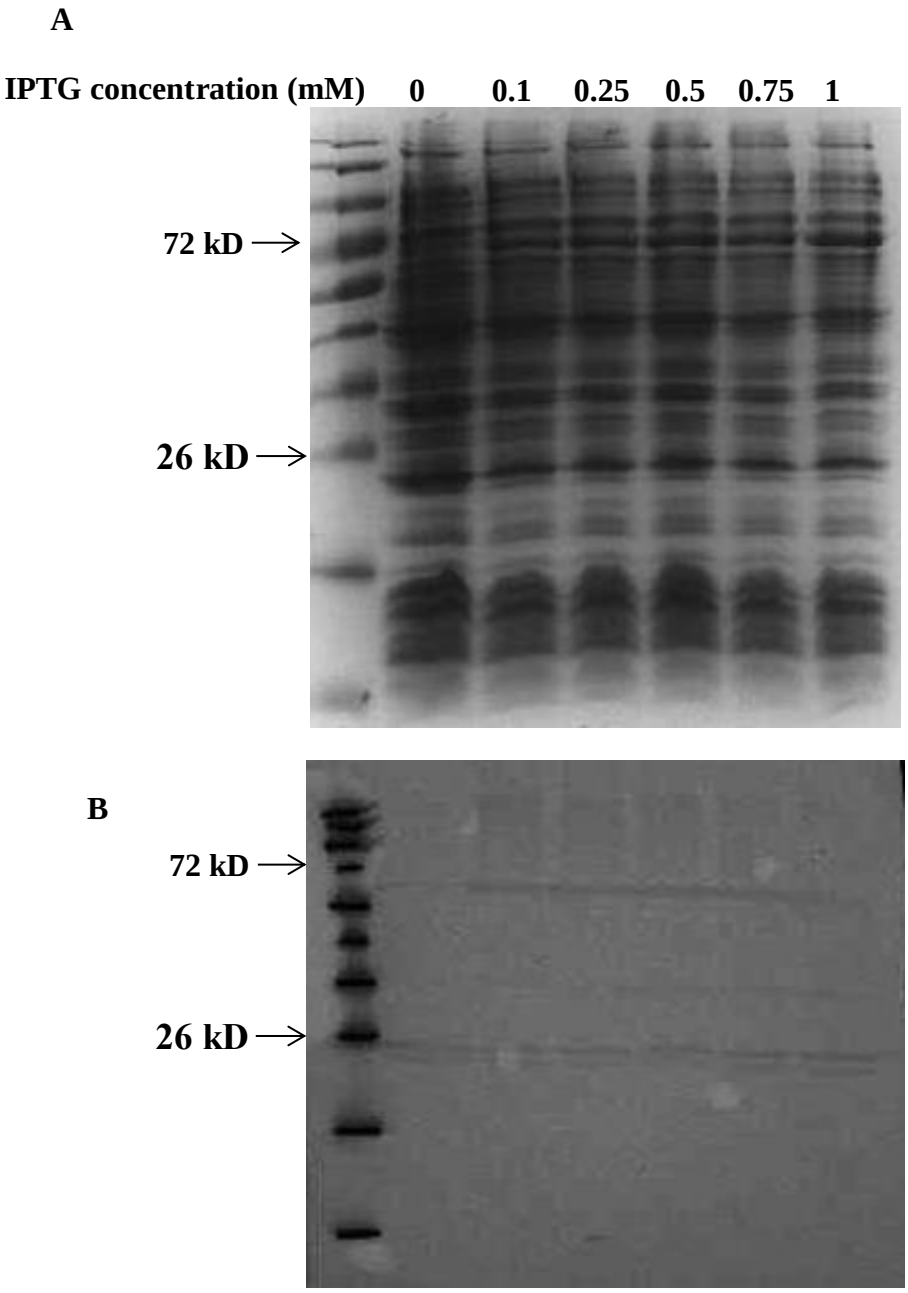

Figure 2.3. Impact of varying concentrations of IPTG on HMGE levels coexpressed with wtEsaR. (A) Coomassie-stained 12% SDS-PAGE gel and (B) western immunoblot of the results are shown. Wild-type protein expression was induced with 0.02% L-arabinose. This titration was not duplicated.

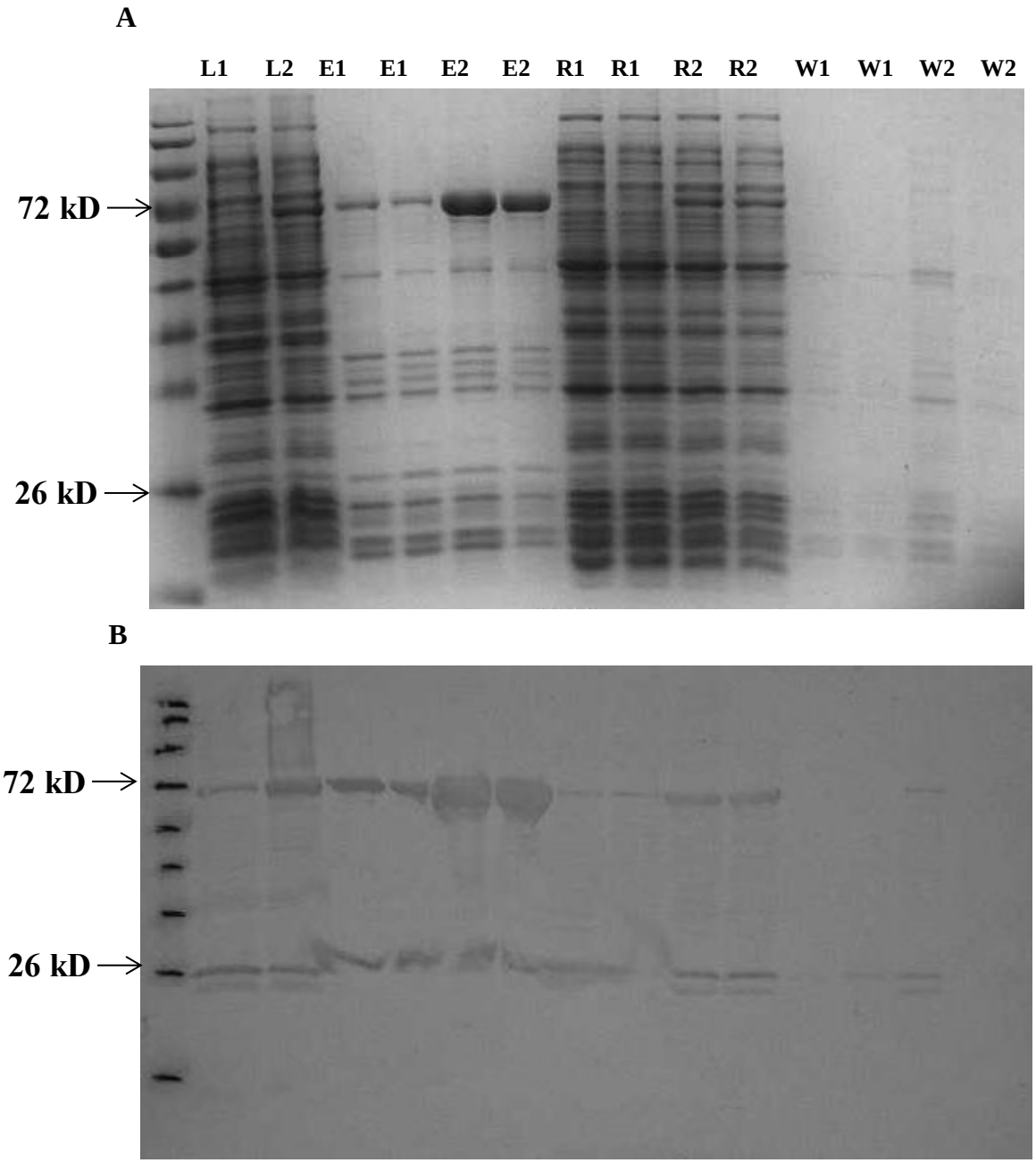

Figure 2.4. SDS-PAGE and western blot analysis of elutants, unbound proteins and washes from manual nickel affinity purifications of lysates containing HMGE and wtEsaR. Manual nickel affinity purification was used to co-purify HMGE and wtEsaR. HMGE expression was either not induced (1) or induced (2) by 1 mM IPTG. Samples were taken from the cell lysates (L) and the elution (after application of Ni elution buffer; E), rinse (protein exiting the column during loading of lysate; R) and wash (during washing of column with Ni binding buffer after loading of lysate; W) steps. Samples were concentrated 80X by TCA precipitation. (A) Coomassie-stained 12% SDS-PAGE gel and (B) western immunoblot of the results are shown. Duplicated results for the elution, rinse and wash were subjected to electrophoresis on the same gels.

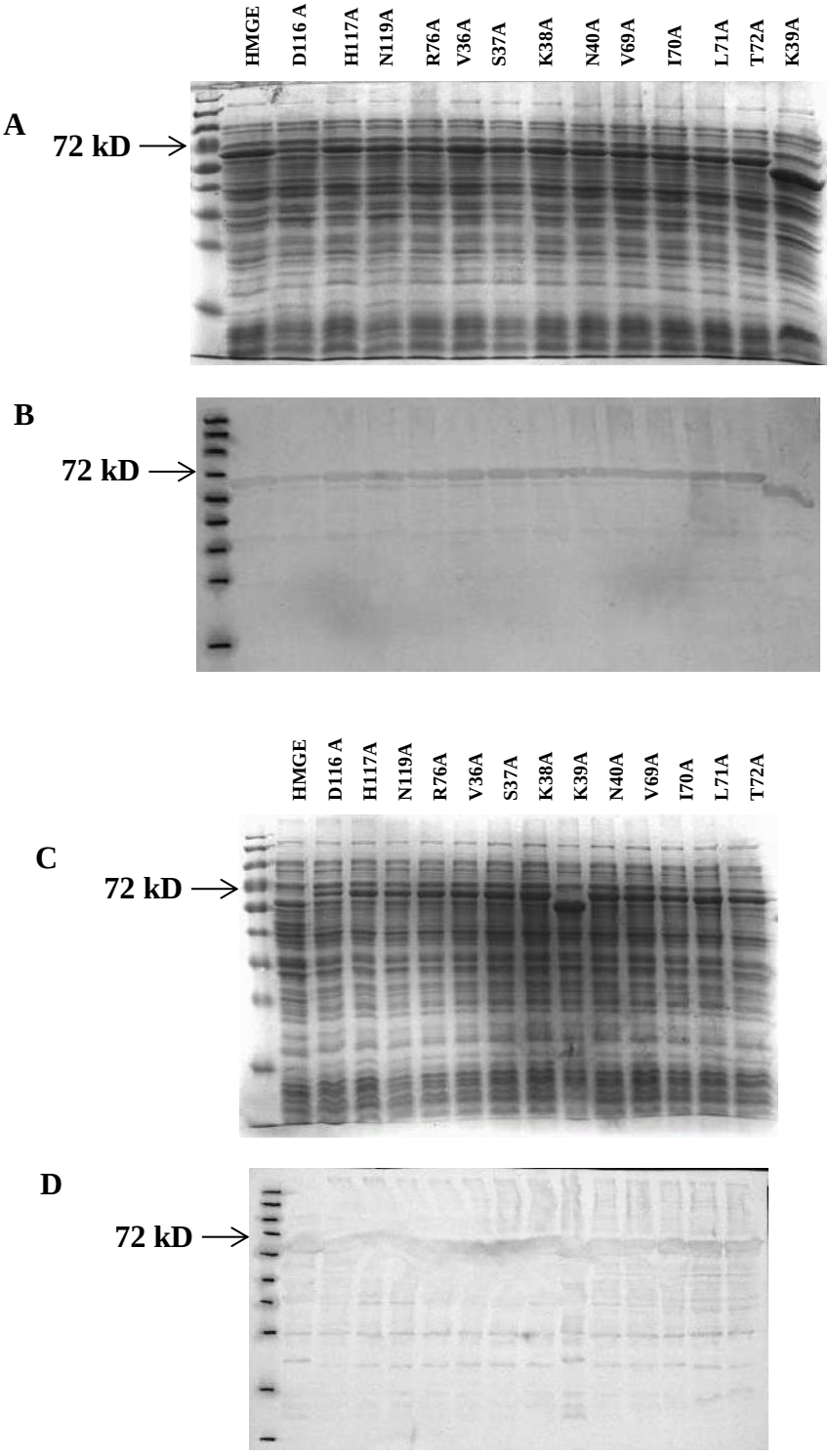

Figure 2.5. Alanine variant HMGE protein intracellular accumulation. (A and C) Coomassie-stained 12% SDS-PAGE gel and (B and D) western immunoblot of whole cell lysates containing alanine variant HMGE proteins are shown. Variant protein expression was induced with 1 mM IPTG. The expected size of HMGE is ~73 kD. Duplicated results are shown.

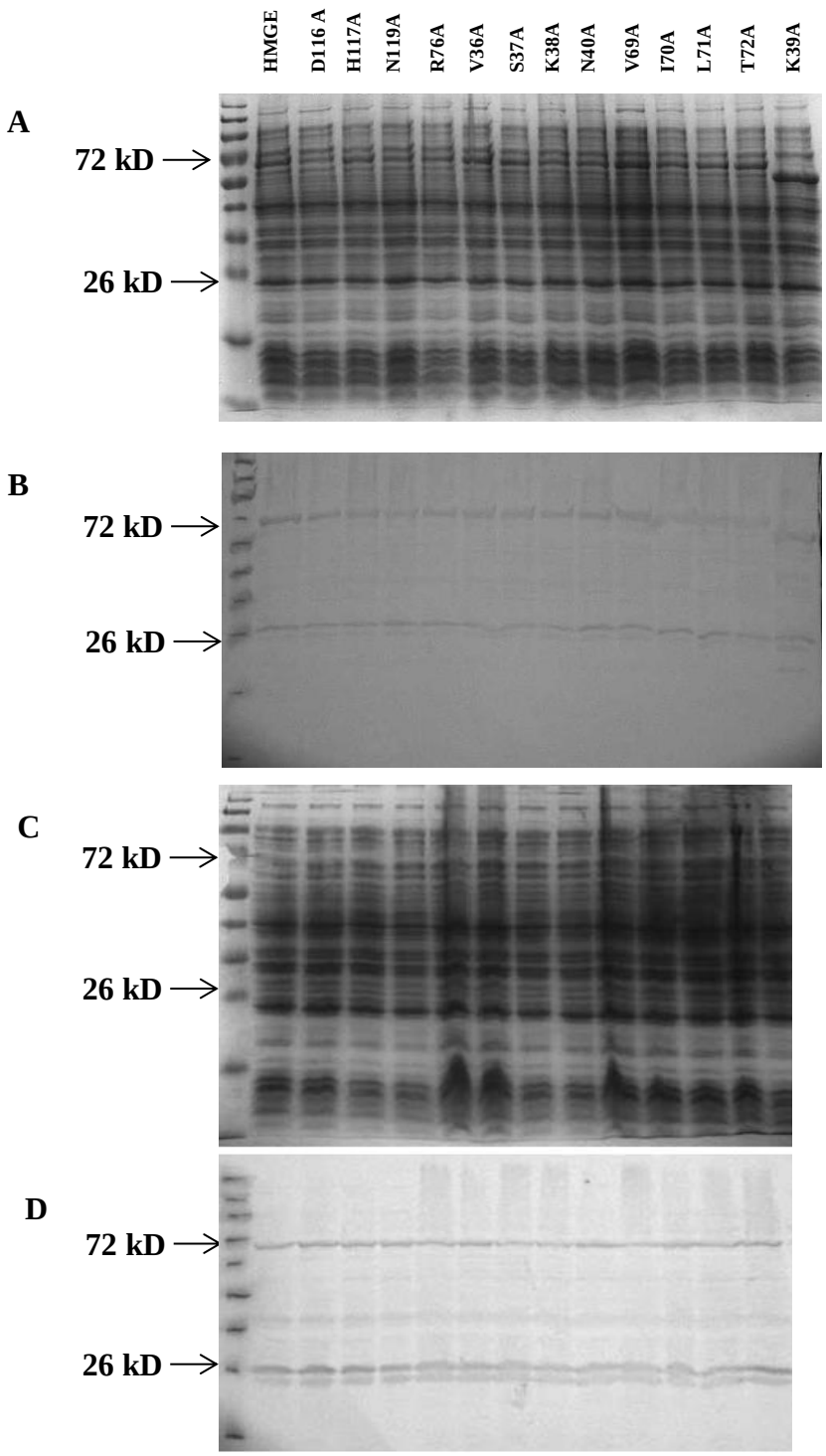

Figure 2.6. Coexpressed wild-type EsaR and HMGE intracellular accumulation. (A and C) Coomassie-stained 12% SDS-PAGE gel and (B and D) western immunoblots of whole cell lysates containing wild-type and variant EsaR proteins are shown. Variant and non-variant HMGE expression was not induced with IPTG. The expected size of wild-type EsaR monomer is ~28 kD. Duplicated results are shown.

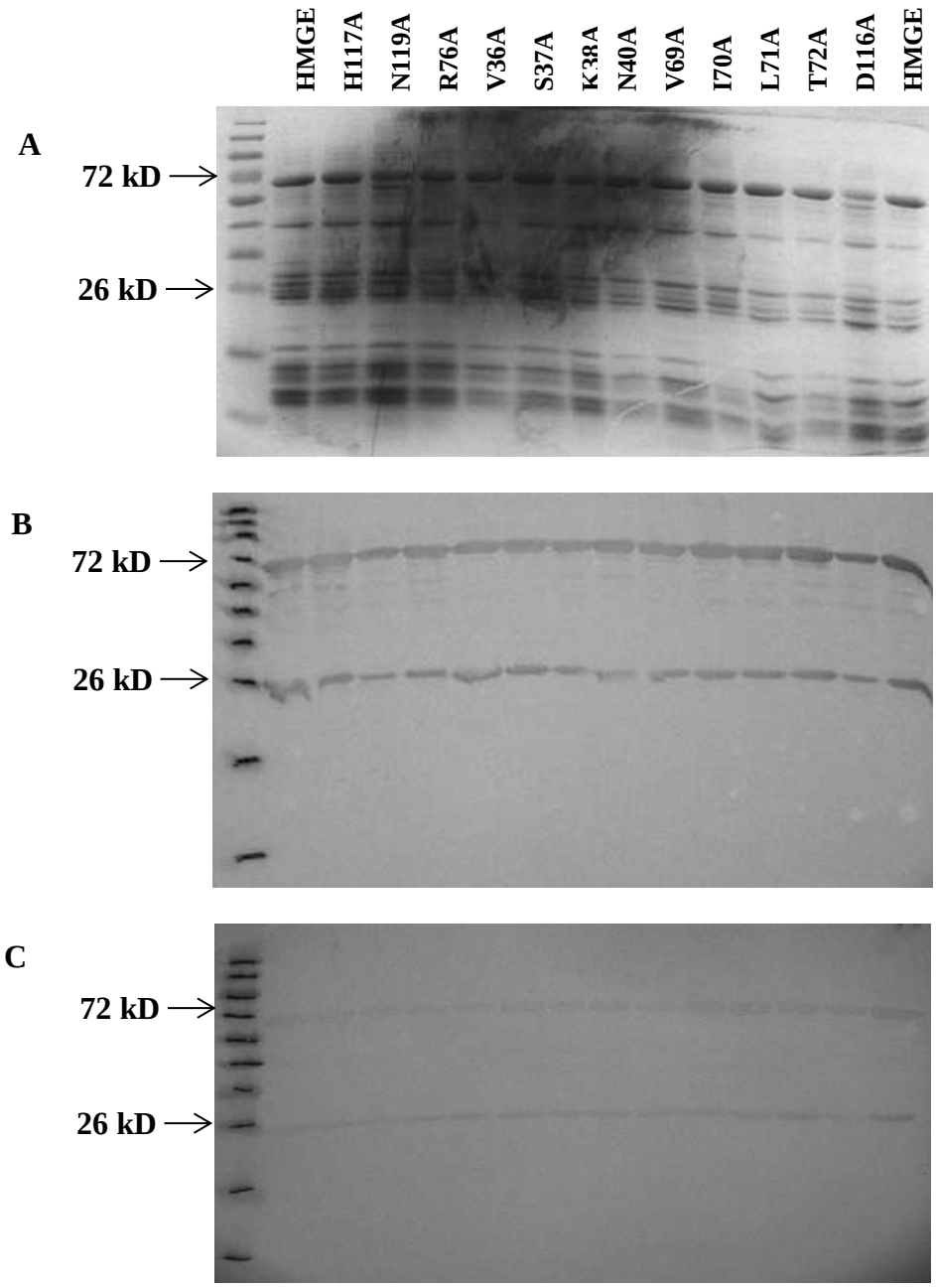

Figure 2.7. Coexpressed heterodimerization assay with alanine substitution variants. (A) Coomassie-stained 12% SDS-PAGE gel and (B and C) western immunoblots of alanine variants assayed for heterodimerization with wtEsaR was shown.

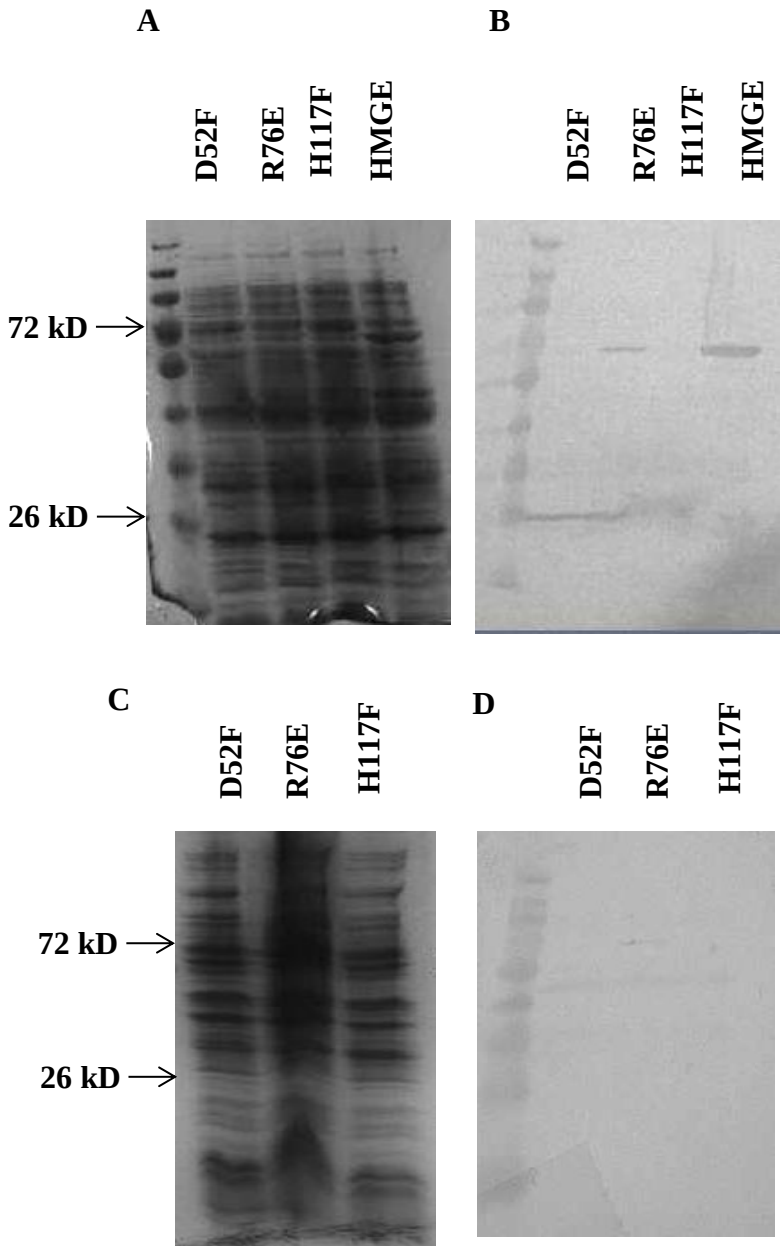

Figure 2.8. Non-alanine variant HMGE protein intracellular accumulation. (A and C) Coomassie-stained 12% SDS-PAGE gels and (B and D) western immunoblots of whole cell lysates containing variant HMGE and wtEsaR proteins are shown. Variant protein expression was induced with 1 mM IPTG. Non-variant HMGE expression was not induced. Wild-type protein expression was induced with 0.02% L-arabinose.

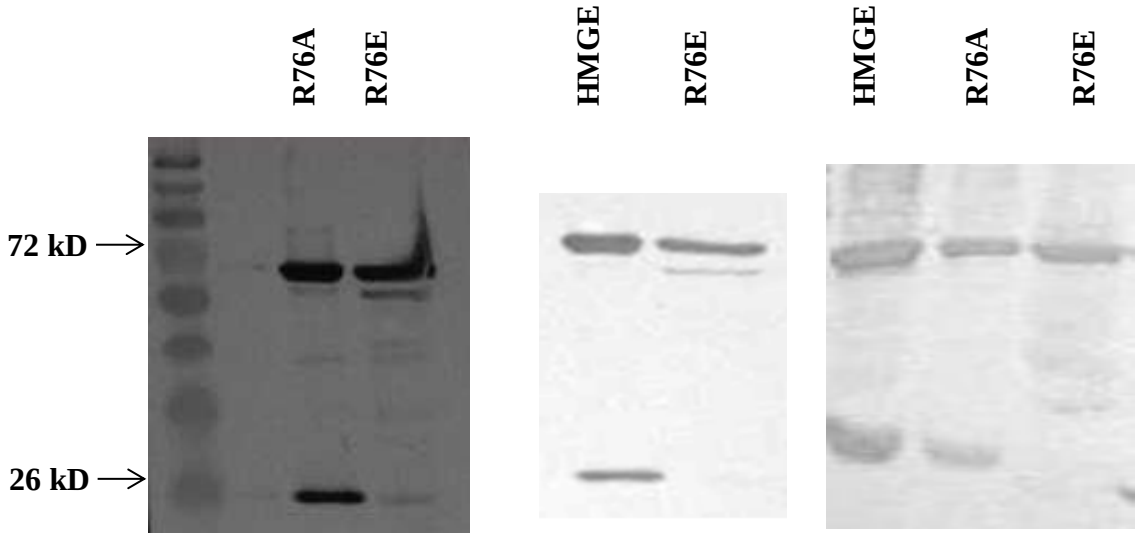

Figure 2.9. Coexpressed heterodimerization coexpression results with HMGE variant R76E. Western immunoblots of the results are shown. The variant R76E seemed unable to complex with wtEsaR as well as HMGE and R76A. Less wtEsaR was co-purified with the variant protein. See Materials and methods for details about sample preparation.

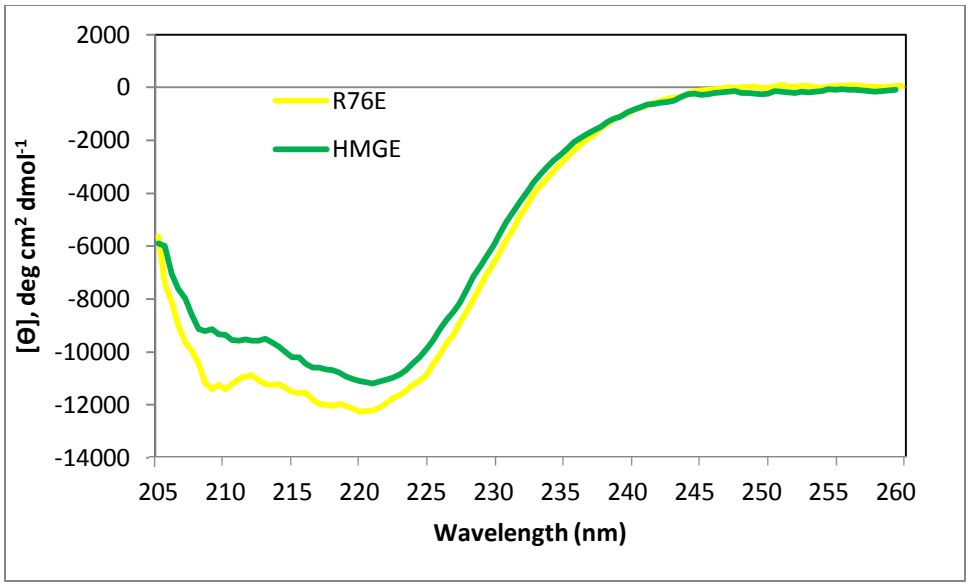

Figure 2.10. Evaluation of HMGE and R76E secondary structure by circular dichroism. Circular dichroism spectroscopy indicates that despite its apparent loss of dimerization ability, R76E still has secondary structures similar to HMGE as indicated by absorption at near UV wavelengths. Proteins with randomized structures do not have strong CD signals in this region. The average results of the duplicated experiments are shown.

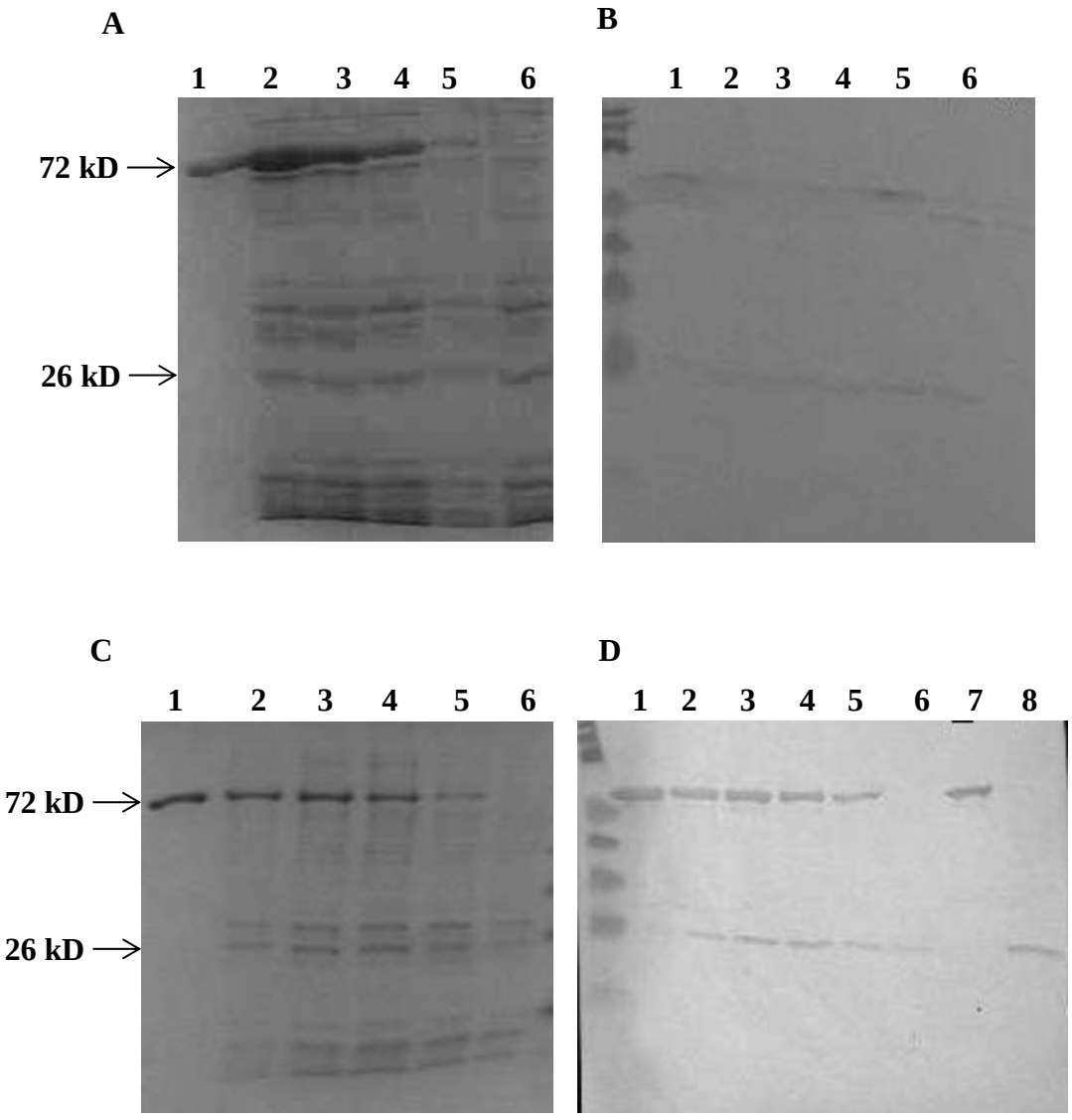

Figure 2.11. Titration of HMGE in coincubation heterodimerization assay. (A and C) Coomassie-stained 12% SDS-PAGE gels and (B and D) western immunoblots are shown. Samples 1 and 7 contained 1000 nM HMGE and no EsaR lysate. Samples 2 through 6 contained, in order, 100µl of 1000 nM, 500 nM, 250 nM, 125 nM and 0 nM HMGE combined with 900 µl EsaR lysate. Sample 8 contained 900 µl EsaR lysate and no HMGE. Samples 7 and 8 were not subjected to nickel affinity purification.

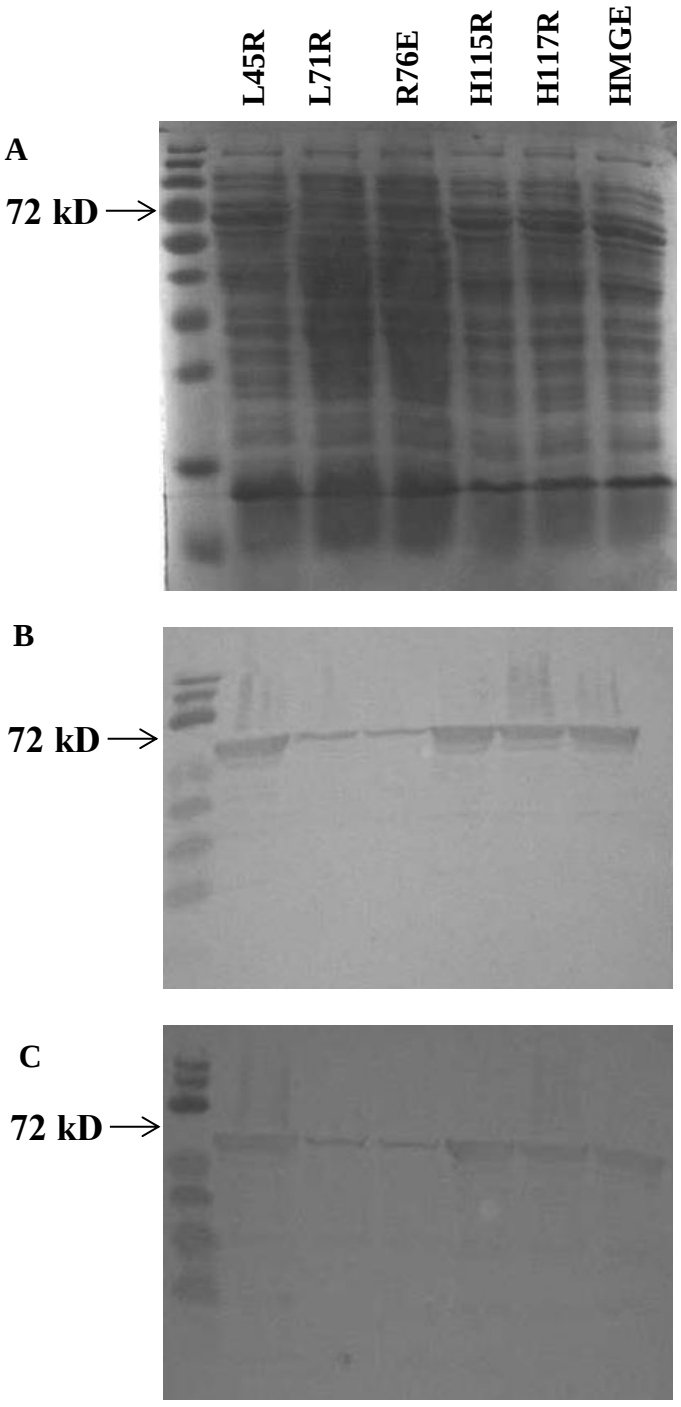

Figure 2.12. Non-alanine variant HMGE intracellular accumulation. (A) Coomassie-stained 12% SDS-PAGE gels and (B and C) western immunoblots of whole cell lysates containing variant HMGE and wtEsaR proteins are shown. Variant and non-variant HMGE protein expression was induced with 1 mM IPTG.

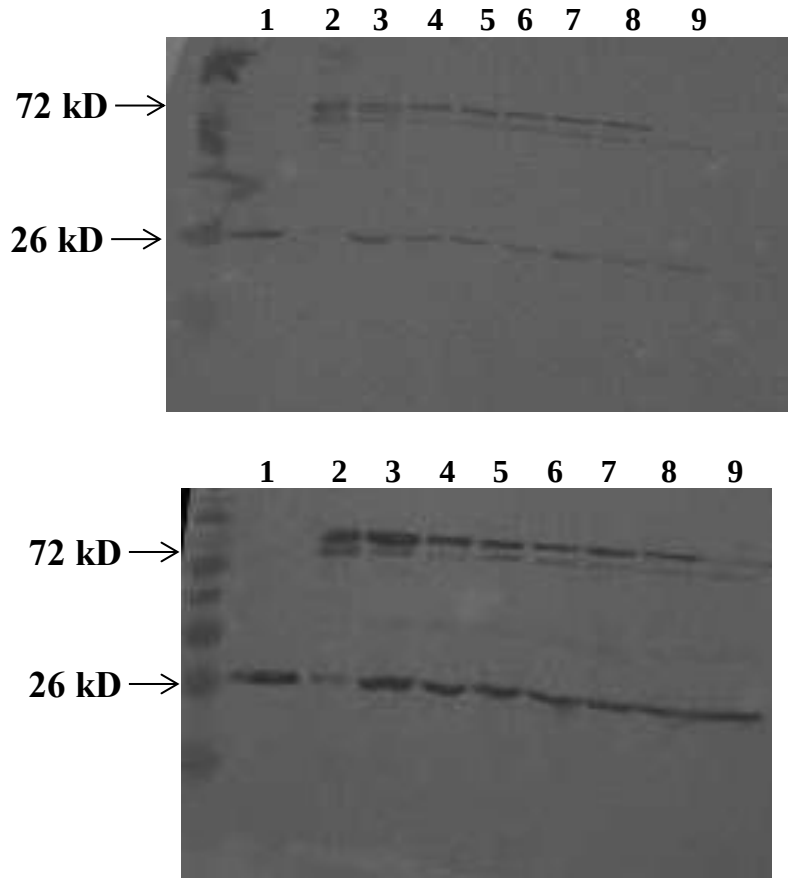

Figure 2.13. Coincubation heterodimerization assay results with non-alanine HMGE variants. Western immunoblots of the results are shown. Controls included a (1) lysate sample containing wtEsaR to show the migration of wtEsaR, (2) a HMGE only sample that was not mixed with wtEsaR lysate and was subjected to nickel affinity purification, and (9) a wtEsaR lysate sample that was subjected to nickel affinity purification. Samples 3 – 8 were, in order, variants L45R, L71R, R76E, H115R and H117R which were mixed with wtEsaR lysate and subjected to nickel affinity purification. The controls only partially worked: wtEsaR was detectable in samples B and I. Duplicated results are shown.

Chapter three

Development of FRET methods for distance estimations between amino acid residues in EsaR

Abstract

Quorum sensing in the corn pathogen *Pantoea stewartii* regulates several genes involved in virulence, surface motility/adherence and stress response. EsaR, a LuxR homologue found in *P. stewartii*, serves as a transcriptional activator and repressor of genes involved in these outputs. High acyl-homoserine lactone (AHL) concentrations at high cell densities result in the inactivation of EsaR. However, the molecular mechanism by which EsaR is inactivated by its cognate AHL ligand is unknown. It was hypothesized that the dimeric protein undergoes a conformational shift in which its two C-terminal domains are spread farther apart from each other, making binding to DNA unfavorable. Focusing on one residue in the N-terminal domain and one residue the C-terminal domain, Förster Resonance Energy Transfer (FRET) methods were developed, which will enable future structural studies.

Introduction

Quorum sensing (QS) in *Pantoea stewartii* is controlled primarily by EsaI and EsaR (1, 2). These proteins respectively synthesize and interact with a small membrane-diffusible acyl-homoserine lactone (AHL) molecule, *N*-(3-oxo-hexanoyl)-L-homoserine lactone. At low cell densities, AHL extra- and intracellular concentrations are also low. EsaR does not bind much ligand. As an apoprotein, EsaR functions as a transcriptional activator and repressor of several genes involved in virulence, surface motility/adherence and stress response (1-6). As the population of *P. stewartii* increases, so does the extra- and intracellular AHL concentration. At a minimum of 2 µM AHL in cell cultures, EsaR binds more of the ligand (2). This leads to an inactivation of the protein.

The response of EsaR and other members of its subfamily to the AHL ligand is unique (7). Most members of the LuxR family are activated by their AHL ligand; some require it to maintain a folded structure. The mechanism by which EsaR is inactivated is unknown. Likewise, it is not known how AHL ligands activate other LuxR homologues. This study could lead not only to an explanation of why the EsaR subfamily behaves differently, but also to a better understanding of how AHL ligands interact with LuxR homologues. It has been hypothesized that a conformational change is induced by the AHL ligand (8). In this study, preliminary Förster Resonance Energy Transfer (FRET) experiments were conducted towards the goal of determining if EsaR undergoes a conformational change when binding to its AHL ligand.

Materials and methods

Bacterial strains, plasmids and growth conditions

Escherichia coli Top10 (Table 3.1) cells were grown, stored and transformed as stated in the Materials and methods section of Chapter Two.

Site-directed mutagenesis

Residues N62, K75, R93, M194 and N227 were selected by F. Schubot (Virginia Tech) for study because they were predicted to be located on the periphery of EsaR by homology models based on QscR from *Pseudomonas aeruginosa* and CviR from C*hromobacterium violaceum* (Fig. 1.3). HMGE (hexahistidine His6, maltose binding protein MBP tagged EsaR) variants N62C, K75C and N227C were generated by site-directed mutagenesis using the Phusion enzyme (New England Biolabs) and pHMGE (Table 3.1). EsaR variants R93C and M194C were generated in the same manner using the plasmid pBAD-EsaR instead of pHMGE (Table 3.1).

Further work to use the genes encoding these two variants to create mutant pHMGE plasmids was not completed. This would have been done using Gateway Cloning to introduce the mutant genes into pDEST-HisMBP, the plasmid from which pHMGE was derived (Table 3.1).

The cysteine variations were necessary for fluorophore labelling (described in the following section). Reaction compositions and thermocycling conditions adhered to the manufacturer's protocol for PCR with the Phusion enzyme except only eighteen cycles were performed with an annealing temperature of 55°C. The primers that were used are detailed in Table 3.2. After the reaction, the methylated non-mutant template was degraded by the addition 1 µl of DpnI to 20 µl of the finished reaction mixture, then incubating for one hour at 37°C. Desired mutations were confirmed as stated in the Materials and methods section of Chapter Two by Sanger sequencing at the Virginia Bioinformatics Institute Core Facility. Variant protein stabilities were analyzed via western immunoblotting using primary antibodies provided by S. B. von Bodman (9).

Protein purification of HMGE cysteine variants

The non-variant HMGE or HMGE cysteine variants were purified by nickel affinity purification from 1 L of cell culture as described in Chapter Two, "Heterodimerization assay – coincubation method". Following this, eluted proteins' buffers were exchanged for HMGE working buffer (500 mM NaCl, 20 mM HEPES, 10% glycerol, pH 7.4) by fast performance liquid chromatography using a 5 ml HiTrap desalting column (GE Healthcare) at 4°C at a maximum rate of 5 ml/min.

Fluorophore labeling of HMGE cysteine variants

Any handling of fluorophore or labeled protein was done in minimal light. The donor fluorophore was Alexa Fluor 488 C5-maleimide; the acceptor, Alexa Fluor 555 C2-maleimide (Table 3.3). The fluorophore reagents were dissolved in water and divided into aliquots containing 0.125 µmol of dye. The solutions were quickly dried by vacuum evaporation by the lab of R. Helm (Virginia Tech) and stored at -70°C.

Overnight labeling at 4°C of the purified proteins was performed by combining 250 µl of a purified cysteine variant (about 20 µM) with an aliquot of a fluorophore dye resulting in a ratio of 25 moles of dye to 1 mole of protein. The following morning, unincorporated dye was removed by buffer exchange into HMGE working buffer with a 50 ml HiPrep 26/10 desalting column (GE Healthcare) at a flow rate of 1 ml/min. Absorptions at 280 nm and the appropriate excitation wavelength for the attached dye were measured. Dye correction factors accounted for the absorbance at 280 nm by the fluorophores using the following equation:

$$c = \frac{A_{280} - A_{dye} \times cf}{\varepsilon_{prot}}$$

in which the protein concentration in molarity (c) is calculated by subtracting the product of the absorbance at the maximum excitation wavelength (A_{dye}) of the fluorophore and its dye correction factor (cf) from the absorbance at 280 nm (A_{280}) and dividing by the molar extinction coefficient of the protein (ε_{prot}).

The concentrations of protein to dye were used to calculate labeling efficiency (ratio of dye concentration to that of protein). The lot data for the fluorophores are detailed in Table 3.3. The excitation and emission spectra of the fluorophores are available on the respective product website pages of the fluorophores (10, 11).

FRET assays, heterodimerization binding curves and distance calculations

Optimization experiments were performed to find concentrations at which donor- and acceptor-labeled proteins would form heterodimers and to find concentrations at which an excess concentration of donor-labeled protein would be saturated by acceptor-labeled protein. All FRET experiments were conducted using black Nunc 96 well plates and a Tecan Infinite M200 plate reader. An integration time of 20 s was allowed. Plate lids were kept off during measurements. A total of 100 µl of sample in each well contained labeled protein in HMGE working buffer. Controls excluding the donor-labeled protein were used to correct for background emission. In each experimental set-up, donor-labeled protein was present at 27 nM. The concentration of acceptor-labeled protein was 0, 4, 12, 24, 48, 96 or 144 nM (Table 3.4).

The excitation wavelength was set to 450 nm and emission wavelengths of 500 to 648 nm (4 nm step size) were measured. Twenty-five measurements were taken at each emission wavelength and averaged. Gains for each assay were calculated by the software (Tecan i-Control, version 1.3.3.0) based on the sample with the highest concentration of donor- and acceptor-labeled proteins. Measurements were taken immediately after mixing, then twice more 1 and 2 hours after mixing before and after the addition of AHL or DNA. The plates were allowed to incubate in the dark at room temperature between measurements. Either 1 µl of AHL (to a final concentration of 1 µM) or 1 µl of DNA (to a final concentration of 2.5 µM) was added to induce conformational changes after the initial three measurements. These AHL and DNA concentrations were used because they were expected to saturate binding to the HMGE variants. J. Geissinger previously found 1 µM AHL to be sufficient *in vitro* (12). The dissociation constant for EsaR-DNA binding is approximately 30 nM (3).

To prepare AHL stocks, AHL was dissolved in acidified ethyl acetate (0.1% acetic acid added). Aliquots were air-dried over several days at -20°C (they could have been more quickly dried at room temperature). DNA stocks were prepared by combining equal concentrations of p*esaR*28F and p*esaR*28R (Table 3.2) and heating them to 95°C in a water bath for 10 min. The water bath was allowed to slowly cool back to room temperature. After reaching room temperature, the newly formed DNA was stored at -20°C.

Averages of both the 1 h and 2 h measurements from repeated experiments were used to construct the binding curves for heterodimerization and to calculate the estimated distances between residues. Experiments were performed in triplicate for FRET assays with AHL and in duplicated for assays with DNA. Curves of heterodimer formation were constructed using a free trial of XLfit version 5.3.1.3, ID Business Solutions Limited. The following formula was used to calculate the dissociation constant:

$$\frac{(A+x+K_D)-\sqrt{(A+x+K_D)^2-4Ax}}{2A}$$

in which A is the concentration of the donor-labeled protein, x is the varied concentration of the acceptor-labeled protein and K_D is the dissociation constant.

Distance calculations were performed using the two equations:

$$E = \frac{R^6}{R^6 + r^6}$$

$$E = 1 - \frac{Fd'}{Fd}$$

in which E is the FRET efficiency, R is the Förster distance in Ångströms, r is the "real" distance in Ångströms, Fd is the relative emission intensity from the donor and Fd' is the relative emission intensity from the donor in the presence of an excess of the acceptor.

Partial *in vitro* proteolysis with thermolysin

In the absence or presence of 67.5 µM AHL, 50 µl of 27 µM non-variant HMGE or the HMGE cysteine variants N62C or N227C in HMGE working buffer was mixed with 50 µl of 144 nM thermolysin (Sigma-Aldrich) in HMGE working buffer with 4 mM $CaCl_2$ added. Immediately after mixing, 20 µl was removed, and the reaction was stopped by adding 0.8 µl of 0.5 M EDTA and 5 µl of 5X sample buffer (v/v 12.48% 1 M Tris pH 6.8, w/v 4% SDS, v/v 20.8% glycerol, v/v 10% β-mercaptoethanol, v/v 5% saturated bromophenol blue solution in water), and boiling for 10 min. The remaining 80 µl of the ongoing reaction was incubated for 1 h at 37°C before stopping the reaction with 3.2 µl of 0.5 M EDTA and 20 µl of 5X sample buffer, and boiling for 10 min. Experiments were duplicated. Except for not using the thermolysin reaction buffer, this procedure followed that used by Schu *et al.* (13). On a 16-lane 12% SDS-PAGE gel, 5 µl of prepared sample was loaded into each well. Gel electrophoresis was performed at 90 V for 2 h.

Results and discussion

FRET assay optimization

FRET assays were used to estimate if the distances between two amino acid residues change between EsaR without AHL (active) and EsaR with AHL (inactive). It was hypothesized that, with the addition of the AHL ligand, distances between residues in the C-terminal domains would increase (Fig. 3.1) (8). HMGE cysteine variants N62C, K75C and N227C were generated and purified by nickel affinity purification. The N62C and K75C variations were located in the N-terminal domain; N227C, in the C-terminal domain. N62C and N227C variants were separately labeled with the donor or acceptor fluorophore, so that there were a total of four

proteins with which to work—either N62C or N227C labeled with either the donor or the acceptor fluorophore. Labeling was completed with 70 to 154% efficiency. Stocks containing 270 nM of protein were aliquoted, flash frozen with liquid nitrogen and stored at -70°C. There was one unsuccessful attempt to label the K75C variant; the labeling efficiency was low. Work with this variant was not continued.

Donor- and acceptor-labeled N227C HMGE were used for optimization of the FRET assay. Fluorophores attached to the proteins were found to be excitable and produced emission spectra in the expected range. It was originally intended to use ~3 nM of donor-labeled protein for the assay, as done by Jing *et al.* (14). However, it was found that at 27 nM, emission from donor-labeled N227C (488-N227C) was more distinct and resulted in smoother (less noisy) spectra (Fig. 3.2). It was also reasoned that using higher protein concentrations would encourage more dimer formation. Using this donor concentration, a titration of acceptor-labeled N227C (555-N227C) concentrations (0 to 144 nM) was performed to determine if 1) dimers would form between differently-labeled monomers and 2) at which concentrations 488-N227C would be saturated with 555-N227C.

Dimer formation was indicated by relative loss of emission from 488-N227C at 520 nm (Fig. 3.3, panels B and D). With increasing amounts of 555-N227C, emission at 520 nm decreased. Heterodimers formed between donor- and acceptor-labeled monomers, bringing the fluorophores close enough to each other to permit FRET. Saturation of 488-N227C was determined by constructing binding curves using the relative emission at 520 nm (Fig. 3.4). Saturation was necessary in case ligand binding affected heterodimerization formation, which would affect the intensity of emission at 520 nm. This effect could be incorrectly interpreted as a change in distance between residues. FRET only occurred when the dyes were attached to the

HMGE proteins. When separate and in the presence of 60 nM non-variant HMGE, the dyes were not capable of producing a FRET signal (Fig. 3.5).

FRET assay with AHL

The addition of the AHL ligand was expected to induce a detectable conformational change in the HMGE protein. Based on the protein structure homology models, the distances between residues in apo- and holo-EsaR were predicted (Table 3.5). Three residue pairs were tested: N62C – N62C, N62C – N227C and N227C – N227C. The calculated experimental distances (Table 3.6) differed from the predictions in two respects: the magnitude of the distance values and the percent change between them.

The calculated distances were larger than the predicted ones (both with and without AHL). This discrepancy could be explained by the use of an imperfect equation for calculating real distances. It was assumed that the selected residues were located on the periphery of the protein and were able to freely and randomly move. If the assumptions were not true or the attached fluorophore hindered movement, then the distance calculations would be incorrect. As the models were only predictions, it was not certain whether the predictions or the experimental results were correct, or if neither was correct. Therefore, the predicted and experimental results were not treated as absolute values. Instead, the primary concern was the percent changes in distances between residues after the addition of AHL.

The greatest changes in distance were predicted to happen between residues in the C-terminal domains of a dimer because of the hypothesized spread between the domains (Fig. 1.3). With the addition of AHL, a 211% increase between the N227 residues on different monomers was expected (Table 3.5). However, none of the three residue pairs showed any significant ($\alpha \leq$

0.05) change in distance after the addition of AHL (Table 3.6). If the hypothesis was correct, then a relatively large increase in distance between N227C residues of different monomers should have occurred. Not obtaining this result led to questions about the initial conformation of HMGE at the start of the assay and about the labeled proteins' abilities to bind AHL.

FRET assay with DNA

Though no AHL was added during cell growth or during the purification process, the possibility that HMGE was already in its inactive form was considered. This would mean that the C-terminal domains of HMGE were already spread apart; the addition of AHL simply locked in place this conformation. It would follow that when interacting to DNA, the conformation of the apoprotein shifts, and the C-terminal domains come together to allow binding to the target DNA sequence. If this were true, then performing the FRET assay with added DNA, instead of AHL, should have yielded changes in the distance. However, such experiments did not indicate any changes in distances between the residues with the addition of DNA (Table 3.7).

The high salt concentration of the HMGE working buffer (500 mM NaCl) may have discouraged DNA binding. The FRET assay with DNA was not repeated with a lower salt concentration. Determining a suitable salt concentration could be done by using an electrophoretic mobility shift assay (EMSA) to confirm that a labeled protein binds to DNA. It should be noted that donor fluorophore fluoresces at the usual 472 nm excitation wavelength used to excite a fluorescein (FAM)-labeled DNA probe used during EMSA analysis. Therefore, other visualization techniques would be needed for evaluating donor-labeled proteins by EMSAs. A different fluorophore could be attached to the DNA probe. Integrated DNA Technologies

offers many other fluorophore modifications of oligonucleotides. Radioactively-labeled probes could also be used.

Partial *in vitro* proteolysis of labeled HMGE with thermolysin +/-AHL

Since no conformational changes were observed in the presence of AHL or DNA, control experiments were performed to determine if the labeled proteins were able to bind AHL. If they were not able to do so, then the predicted conformational shift would not occur, and the distances would not change. Partial *in vitro* proteolysis with thermolysin was used to determine how well the labeled proteins bound AHL. In the presence of AHL, HMGE is partially protected from degradation by thermolysin (13). Attempts to regenerate the partial proteolysis results obtained by Schu *et al.* produced differential banding patterns. However, these patterns were not the same as those previously observed (Fig. 3.6, panel A, lanes -AHL 1' and +AHL 1').

The results indicated that the proteins labeled for FRET analysis were not able to bind AHL well. Compared to HMGE, the labeled proteins were more easily degraded by thermolysin in the presence of AHL (Fig. 3.6, panels B and C, lanes 488 +AHL 1' and lanes 555 +AHL 1'). The labeled N62C proteins seemed to be better protected from degradation than the labeled N227C proteins, as indicated by the darker bands at 72 kD. The results could be explained by three possibilities.

First, the proteins were not able to bind AHL. If the labeled proteins did not bind the available AHL, then they would not receive the same protection from degradation. Second, the proteins were able to bind AHL when they were first purified, but have since lost that ability. This could provide an explanation for why the labeled N62C proteins (Fig. 3.6, panel B) were better protected from proteolysis by AHL than the labeled N227C proteins (Fig. 3.6, panel C).

The N62C variant was purified about three months after N227C was, but all labeled variants were analyzed in the limited proteolytic assay on the same day, along with the control non-variant HMGE protein. Third, the proteins do bind AHL, but in a different manner than HMGE does. This could be addressed by performing the "*in vitro* AI binding assay" established by D. Schu to determine how well the labeled variants bind the ligand (15). If bound AHL were extractable, it would suggest that the protein did bind AHL. It just did so in a fashion that did not provide much protection from thermolysin.

Conclusions

The methods for generating, purifying and labeling the cysteine variants and performing the FRET assay with AHL were developed. A few more controls and trial experiments are needed. Primarily, the HMGE cysteine variants N62C and N227C should be repurified, relabeled and retested. The abilities of these proteins to bind AHL should be evaluated by partial *in vitro* proteolysis before performing the FRET assay with AHL.

Addition of bovine serum albumin (BSA) or non-variant HMGE to experimental samples could be used to verify specific formation of heterodimers. Loss of FRET with the addition of BSA would indicate that the labeled proteins non-specifically interact with other proteins. If the FRET signal remains the same in the presence of BSA but decreases if non-variant HMGE is added, then this would suggest a specific interaction between the labeled protein and other HMGE proteins. Overall, using more recently purified proteins and properly controlled experiments will afford more confidence in future results from this FRET assay.

Acknowledgements

We thank the lab of R. Helm for performing vacuum evaporation for preparation of fluorescent dye stocks. We are also grateful to F. Schubot for his work and assistance with protein modeling, and FRET experimental design and interpretations. Funding for this work was supplied by grant MCB-0919984 from the National Science Foundation, the Virginia Tech Graduate Research and Development Fund, and support from the Lewis Edward Goyette Graduate Fellowship.

References

1. Beck von Bodman S, Farrand SK. 1995. Capsular polysaccharide biosynthesis and pathogenicity in *Erwinia stewartii* require induction by an N-acylhomoserine lactone autoinducer. *J Bacteriol* 177:5000-8.
2. von Bodman SB, Majerczak DR, Coplin DL. 1998. A negative regulator mediates quorum-sensing control of exopolysaccharide production in *Pantoea stewartii* subsp. *stewartii*. *Proc Natl Acad Sci U S A* 95:7687-92.
3. Minogue TD, Wehland-von Trebra M, Bernhard F, von Bodman SB. 2002. The autoregulatory role of EsaR, a quorum-sensing regulator in *Pantoea stewartii* ssp. *stewartii*: evidence for a repressor function. *Mol Microbiol* 44:1625-35.
4. Minogue TD, Carlier AL, Koutsoudis MD, von Bodman SB. 2005. The cell density-dependent expression of stewartan exopolysaccharide in *Pantoea stewartii* ssp. *stewartii* is a function of EsaR-mediated repression of the *rcsA* gene. *Mol Microbiol* 56:189-203.
5. Carlier AL, von Bodman SB. 2006. The *rcsA* promoter of *Pantoea stewartii* subsp. *stewartii* features a low-level constitutive promoter and an EsaR quorum-sensing-regulated promoter. *J Bacteriol* 188:4581-4.
6. Ramachandran R, Stevens AM. 2013. Proteomic analysis of the quorum-sensing regulon in *Pantoea stewartii* and identification of direct targets of EsaR. *Appl Environ Microbiol* 79:6244-52.
7. Stevens AM, Queneau Y, Soulere L, von Bodman S, Doutheau A. 2011. Mechanisms and synthetic modulators of AHL-dependent gene regulation. *Chem Rev* 111:4-27.
8. Chen G, Swem LR, Swem DL, Stauff DL, O'Loughlin CT, Jeffrey PD, Bassler BL, Hughson FM. 2011. A strategy for antagonizing quorum sensing. *Mol Cell* 42:199-209.
9. Schu DJ, Carlier AL, Jamison KP, von Bodman S, Stevens AM. 2009. Structure/function analysis of the *Pantoea stewartii* quorum-sensing regulator EsaR as an activator of transcription. *J Bacteriol* 191:7402-9.
10. Life Technologies. 2013. Alexa Fluor® 488 C5 Maleimide. https://www.lifetechnologies.com/order/catalog/product/A10254?ICID=search-product [accessed Dec. 4, 2013].
11. Life Technologies. 2013. Alexa Fluor® 555 C2 Maleimide. https://www.lifetechnologies.com/order/catalog/product/A20346?ICID=search-product [accessed Dec. 4, 2013].
12. Jing X, Jaw J, Robinson HH, Schubot FD. 2010. Crystal structure and oligomeric state of the RetS signaling kinase sensory domain. *Proteins* 78:1631-40.
13. Schu DJ. 2009. Structure/function analysis of the quorum-sensing regulator EsaR from the plant pathogen *Pantoea stewartii*. *Ph.D. Thesis. Virginia Tech, Blacksburg.*
14. von Bodman SB, Ball JK, Faini MA, Herrera CM, Minogue TD, Urbanowski ML, and Stevens AM. 2003. The quorum-sensing negative regulators EsaR and $ExpR_{ECC}$, homologues within the LuxR family, retain the ability to function as activators of transcription. *J. Bacteriol* 185:7001-7.
15. Zhang RG, Pappas KM, Brace JL, Miller PC, Oulmassov T, Molyneaux JM, Anderson JC, Bashkin JK, Winans SC, Joachimiak A. 2002. Structure of a bacterial quorum-sensing transcription factor complexed with pheromone and DNA. *Nature* 417:971-4.

Tables and figures

Table 3.1. Plasmids and strains used in this study.

Plasmid/Strain	Relevant Information	Reference(s)
pHMGE	*attb*-His_6-MBP-TEV-Gly_5- *esaR-attb* under P_{tac}, Amp^r, derived from pDEST-HisMBP	(13)
pN62C	Mutant pHMGE encoding variant N62C HMGE	This study
pK75C	Mutant pHMGE encoding variant K75C HMGE	This study
pN227C	Mutant pHMGE encoding variant N227C HMGE	This study
pBAD-EsaR	*esaR* ligated into *Eco*RI sites in pBAD22, 15 bp carryover of pGEM vector, Amp^r	(16)
pBAD-R93C	Mutant pBAD-*esaR* encoding variant R93C	This study
pBAD-M194C	Mutant pBAD-*esaR* encoding variant M194C	This study
***E. coli* Top10**	Commercially available from Life Technologies	(17)

Table 3.2. Primers used in this study.

Primer[a]	Sequence[b]	T_m (°C)
	Site-directed mutagenesis primers	
N62CF	GGATTAGGTTATACCGCGCTAACTGCTTTCAGCTGACCG	66.4
N62CR	CGGTCAGCTGAAAGCAGTTAGCGCGGTATAACTAATCC	66.4
K75CF	GTTATTCTCACGGCCTTTTGCCGCACCTCGCCGTTT	69.3
K75CR	AAACGGCGAGGTGCGGCAAAAGGCCGTGAGAATAAC	69.3
R93CF	ACGCTGATGTCCGACCTGTGCTTCACCAAAATTTTCTCT	65.5
R93CR	AGAGAAAATTTTGGTGAAGCACAGGTCGGACATCAGCGT	65.5
M194CF	GGTGTTGTACTGGGCGAGTTGCGGCAAAACCTATGCTG	68.8
M194CR	CAGCATAGGTTTTGCCGCAACTCGCCCAGTACAACACC	68.8
N227CF2	AAACTGGGCGTCAGTTGCGCCCGACAGGCTATC	70.7
N227CR2	GATAGCCTGTCGGGCGCAACTGACGCCCAGTTT	70.7
	Sequencing primers	
tacF	TGACAATTAATCATCGGCTCGTATAATGT	56.4
tacHM_rev	GGAACGCTTTGTCCGGGGTGATTTCAGC	65.1
N40AF	GATTACGCTTACACTGTTGTGAGCAAAAAAGCTCCTTCAAATGTTCT GATTAT	65.1
L71AR	GTTTAAAGGCCGTGGCAATAACCGGATCGGTCAGCTGAAAG	67.7
	FRET assay with DNA primers	
p*esaR*28F	TCTTGCCTGTACTATAGTGCAGGTTAAG	57.8
p*esaR*28R	CTTAACCTGCACTATAGTACAGGCAAGA	57.8

[a] Site-directed mutagenesis primers were named with the original residue identity (using single letter code), position, resulting variation and forward (F) or reverse (R).

[b] Underlines indicate the altered codons for mutagenesis.

Table 3.3. Lot data for donor and acceptor fluorophores.[a]

Fluorophore	Max. absorption wavelength	Extinction coefficient	Dye correction
Alexa Fluor 488 C5-maleimide	493 nm	70000 cm^{-1} M^{-1}	0.11
Alexa Fluor 555 C2-maleimide	557 nm	163000 cm^{-1} M^{-1}	0.08

[a]This information was provided on the manufacturer's website (Life Technologies).

Table 3.4. FRET assay experimental set-up.[a]

Sample No.	1	2	3	4	5	6	7	8	9	10	11	12	13	14
488-protein (nM)	0	0	0	0	0	0	0	27	27	27	27	27	27	27
555-protein (nM)	0	4	12	24	48	96	144	0	4	12	24	48	96	144

[a]For each performance of the FRET assay, samples containing donor- (488) and/or acceptor- (555) labeled protein were organized on a microtiter plate in a consistent fashion. The controls for background fluorescence, samples 1 – 7 were placed, in order, in the same one row. Samples 8 – 14 formed a second row.

Table 3.5. Predicted intermolecular distances between the α-carbons of residues in EsaR in the absence and presence of AHL.[a]

Residue	N62'		K75'		R93'		M194'		N227'	
	-AHL	+AHL	-AHL	+AHL	-AHL	+AHL	-AHL	+AHL	-AHL	+AHL
N62	47	58	32	45	50	65	24	12	34	25
K75	31	45	21	32	38	52	21	46	26	35
R93	48	66	39	52	56	74	34	22	37	35
M194	24	12	21	46	34	22	14	62	7	53
N227	34	25	26	35	37	35	8	62	17	53

[a] Values are in terms of Ångströms (table provided by F. Schubot).

Table 3.6. Average calculated distances between residues by FRET assay with AHL.[a]

Residue	N62'			N227'		
	-AHL	+AHL	*p*-value	-AHL	+AHL	*p*-value
N62	83	91	0.086	66	63	0.83
N227	66	63	0.83	63	66	0.21

[a]The experiments were performed in triplicate. Using Microsoft Excel, two-tailed paired *t*-tests were performed to compare the average distances between a pair of residues in the absence and presence of AHL. The significance level was set at 0.05. Distance values are in terms of Ångströms.

Table 3.7. Average calculated distances between residues by FRET assay with DNA.[a]

Residue	N62'		N227'	
	-DNA	+DNA	-DNA	+DNA
N62	76	80	64	65
N227	64	65	65	62

[a]The experiment was duplicated. Values are in terms of Ångströms.

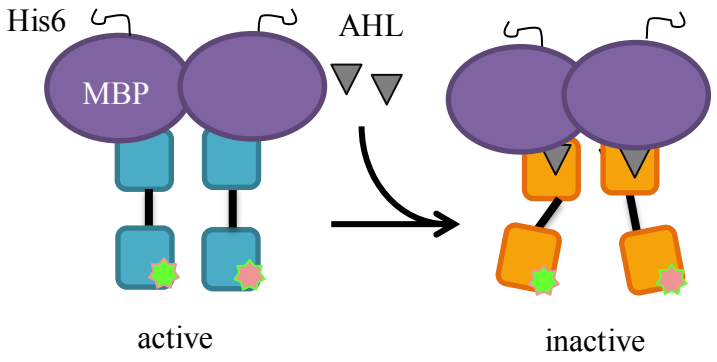

Figure 3.1. Cartoon model of FRET assay. HMGE protein with differentially labeled monomers are presented with ligand. Changes in distances will be detected if they are large enough.

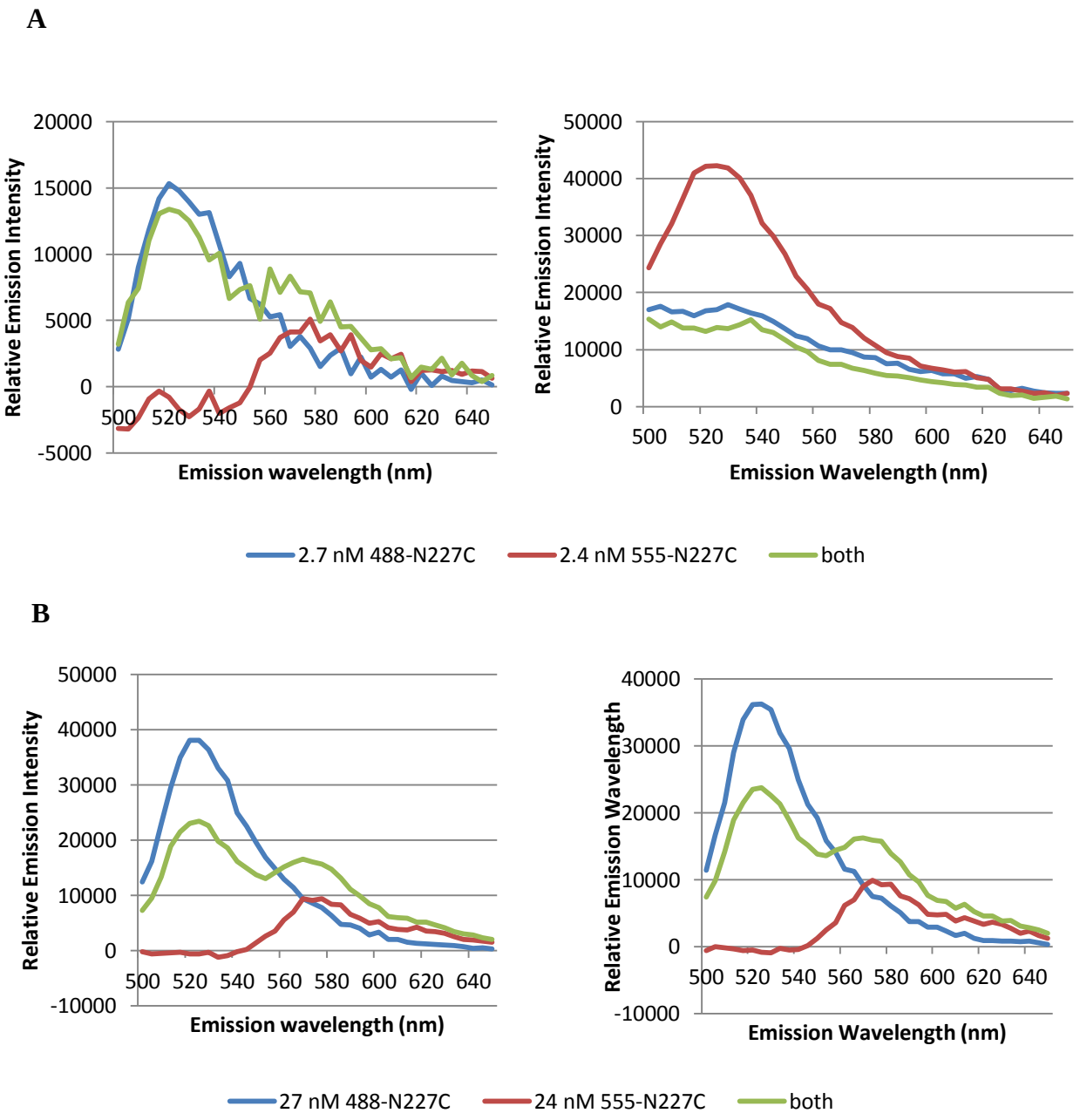

Figure 3.2. Determination of labeled protein concentrations for FRET assay. Using samples containing (A) 2.7 and 2.4 nM of labeled N227C protein and (B) 27 or 24 nM of labeled N227C protein, emission measurements were taken after excitation at 450 nm. Using the higher concentrations of protein yielded more consistent results. The inconsistency shown in panel A could have been caused by pipetting errors. Data was collected 1 h after mixing the proteins together. Duplicated results are shown.

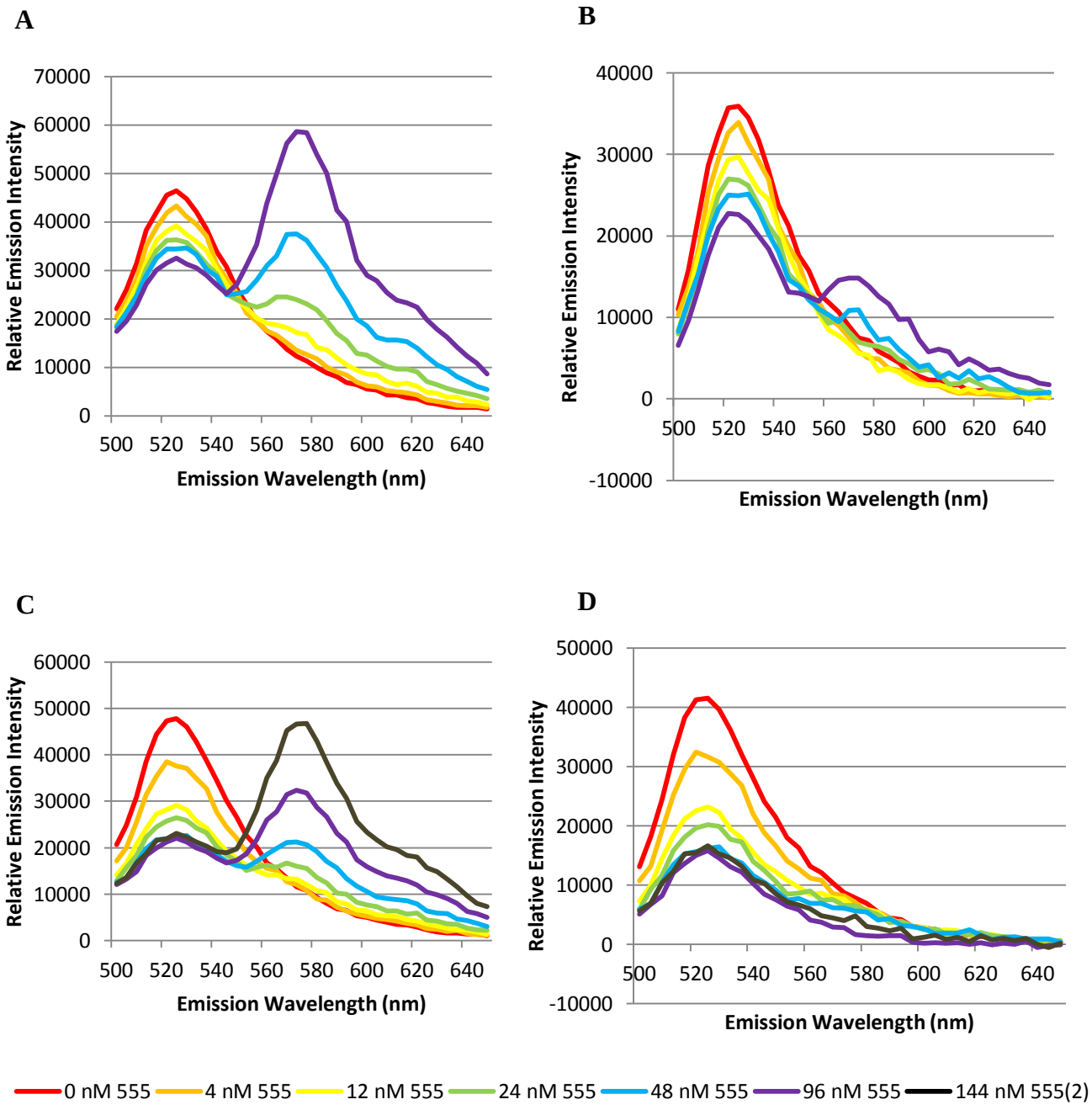

Figure 3.3. Donor emission quenching during FRET analysis of 488-N227C and 555-N227C. Raw data (A and C) and data corrected for background fluorescence (B and D) are shown. Donor and acceptor emissions form two distinct peaks (at 520 and 580 nm, respectively) in the spectra. In the presence of higher amounts of acceptor (555), donor emission decreases, and acceptor emission increases. Data was collected 1 h after mixing the proteins together. Duplicated results are shown.

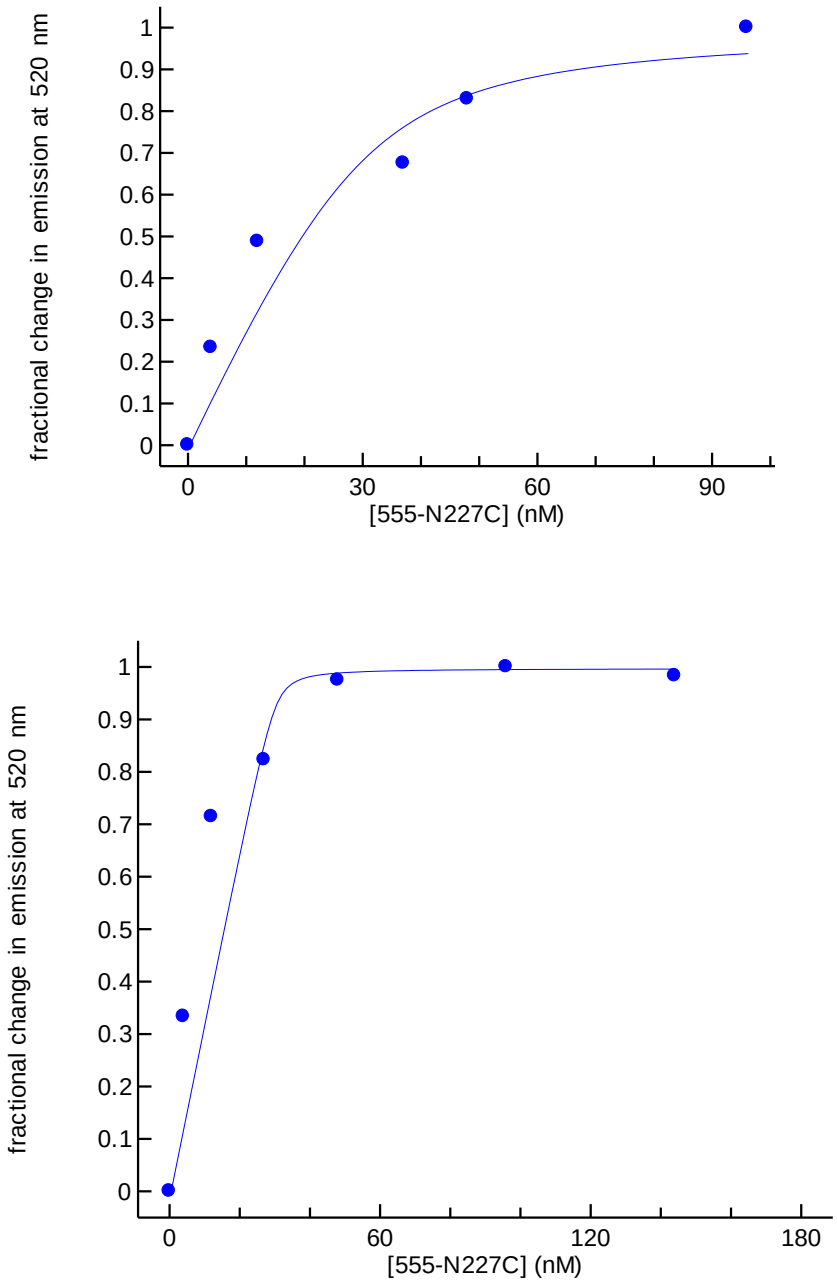

Figure 3.4. Saturation of heterodimer formation between 488-N227C and 555-N227C. Using donor emission intensities at 520 nm, binding curves for the formation of heterodimers between 488-N227C and 555-N227C was constructed to determine the acceptor concentration at which the donor is saturated. Graphs were made using a free trial of XLfit version 5.3.1.3, ID Business Solutions Limited. Data was collected 1 h and 2 h after mixing the proteins together, then averaged. Duplicated results are shown.

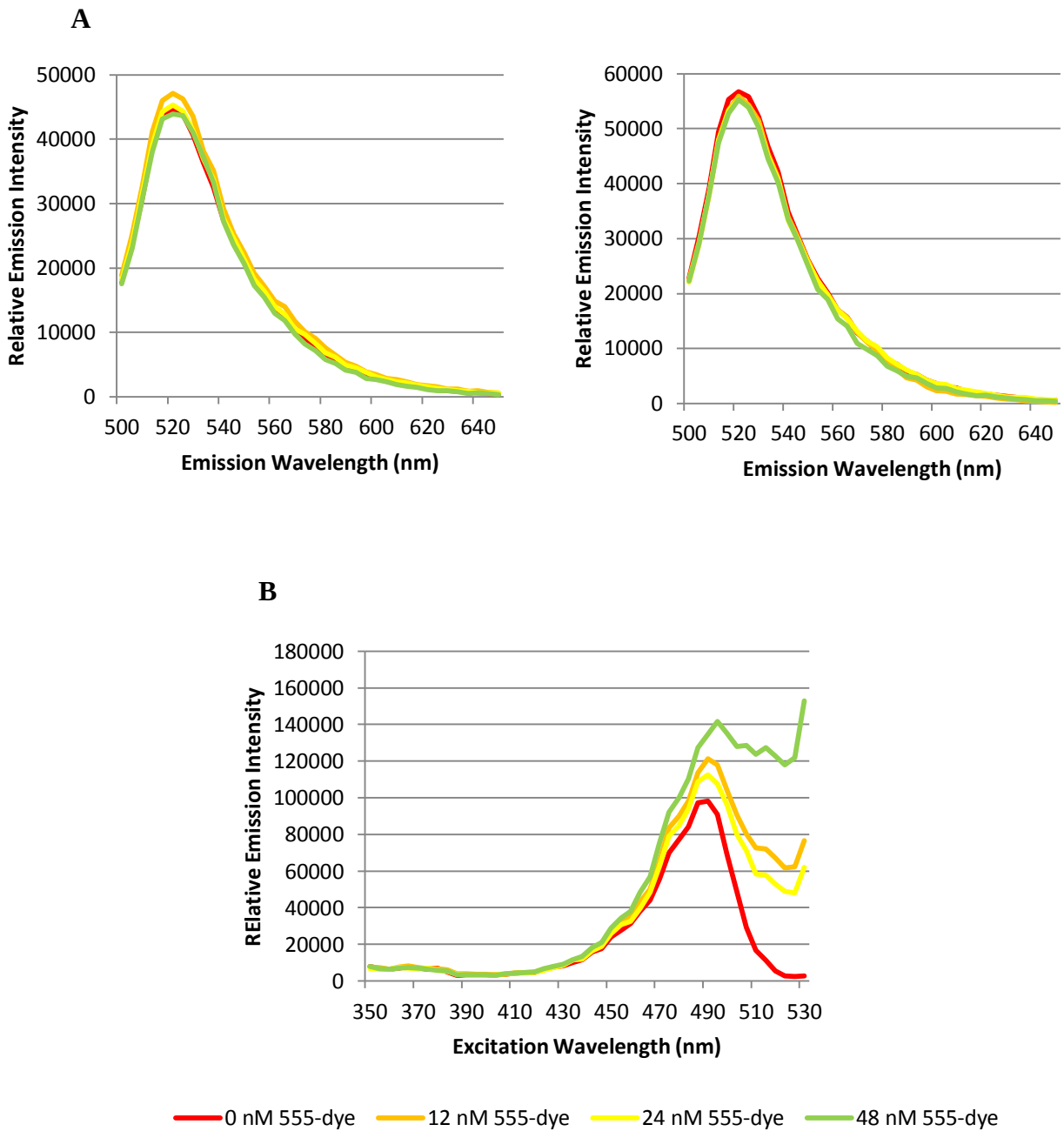

Figure 3.5. Lack of FRET without labeled proteins. Without attachment to HMGE proteins, the donor and acceptor dyes alone were not able to stay close to each other and allow FRET to occur. (A) This is shown by the lack of emission at 572 nm by the acceptor fluorophore (555-dye) and by the steady relative emission at 520 nM by donor fluorophore despite increasing 555-dye concentrations. Donor fluorophore concentrations were held at 27 nM while that of the acceptor varied. Duplicated results are shown. (B) One set of samples was excited at along a range of wavelength (350 – 530) nm to ensure that the acceptor fluorophore was excitable. The relative emission intensity at 570 nm was measured.

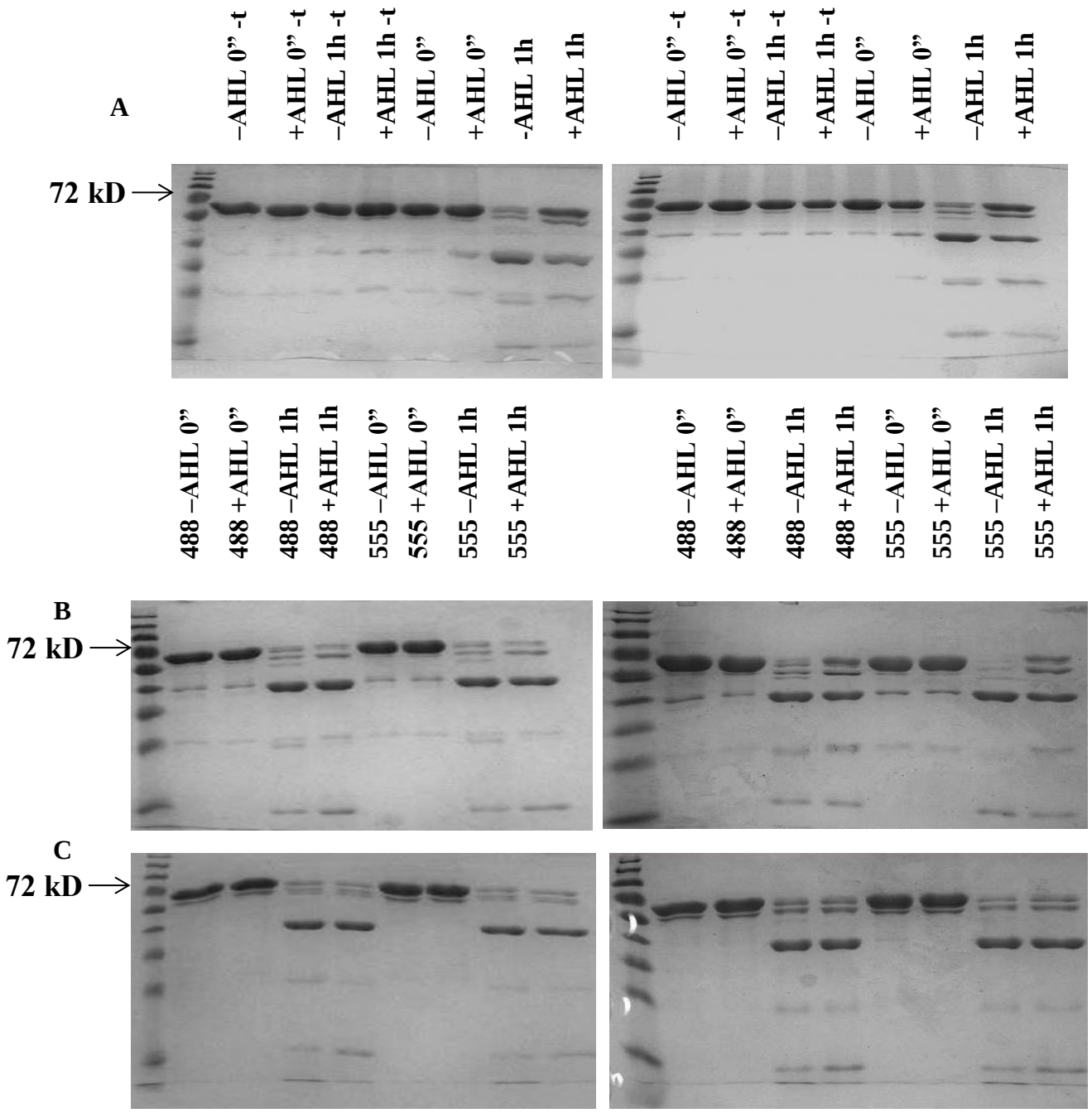

Figure 3.6. Partial thermolysin digestion of HMGE and fluorophore-labeled HMGE in the absence and presence of AHL. Coomassie-stained 12% SDS-PAGE gels are shown. Partial *in vitro* proteolysis of (A) non-variant HMGE, (B) donor (488)- and acceptor (555)-labeled N62C and (C) donor (488)- and acceptor (555)-labeled N227C was performed. Each reaction was either immediately stopped (0”) or incubated at 37°C for 1 h (1h) in the absence or presence of AHL (-/+AHL). Samples containing the non-variant HMGE protein were also incubated without added thermolysin (-t). Duplicated results are shown.

Chapter four

Overall conclusions and appendix

Concluding remarks

The structure of EsaR and the mechanism of how it responds to its cognate AHL molecule are unknown. Using a soluble and biologically relevant fusion protein, HMGE, experimental methods for studying structural aspects of EsaR were developed. The primary purposes of these methods were to determine the dimerization interface of EsaR and to assess the possibility of a conformational shift in response to ligand.

EsaR is suspected to function as a dimer (1). Other LuxR homologues have also been found to have dimeric structures, yet each structure is distinctive (symmetric versus asymmetric arrangements) (2-4). The dimerization interface is, therefore, an important aspect of the structure and function of EsaR. To understand the construction of the dimer, two heterodimerization assays were designed to characterize individual amino acids for their importance in dimer formation. Amino acid residues (V36, S37, K38, K39, N40, L45, V69, I70, L71, T72, R76, D116, H115, H117 and N119) were selected by homology modeling. A combination of alanine and non-alanine substitutions of these residues were tested by the heterodimerization assays.

One HMGE variant, R76E, was tested by both heterodimerization assays (coexpression and coincubation), yielding different results. The result from the coexpression assay could be interpreted two ways: either the amino acid residue R76 might be involved in dimerization of EsaR, or the lower intracellular accumulation of R76E HMGE did not allow for *in vivo* oligomerization with EsaR. The coincubation assay indicated that R76E HMGE might be able to stably interact with EsaR. However, the experimental results from the coincubation assay were inconclusive as the controls for the assay did not produce the expected results. The conflicting results of the two assays indicated that the assays require further optimization to eliminate non-

specific interactions not only between proteins but also between untagged samples and the affinity purification columns before any biological conclusions can be drawn.

The multimeric state of EsaR does not seem to change in the presence of AHL; however, there is some evidence that the overall conformation may shift (1). Noticing how an antagonistic AHL molecule affected the structure of CviR from *Chromobacterium violaceum*, Chen *et al.* proposed that EsaR undergoes a similar conformational shift when bound to its AHL ligand (4). To test this, Förster resonance energy transfer **(**FRET**)** experiments were developed. These experiments sought to use the FRET phenomenon that occurs between chromophores in close proximity to one another to measure the distances between EsaR residues in the absence and presence of AHL.

The FRET assay was optimized and tested with two cysteine-substituted and fluorophore-labeled residues, N62C and N227C. The tests did not indicate any changes in the distances between residues on different subunits when either AHL or DNA was added. These results could have been caused by the labeled proteins not being able to bind either AHL or DNA. Control experiments performed to address this concern suggested that the labeled proteins did not bind AHL as well as HMGE.

These studies laid some foundation for studying the structural aspects of EsaR. With working controls, heterodimerization assays can be used to characterize different amino acids for their respective roles in oligomerization. The FRET experiments can be redone with freshly purified protein and with other HMGE proteins fluorescently labeled at other amino acid residues. Further modifications to the methods and use of the control experiments as described in the previous chapters would be beneficial in future work.

Appendix

Work was conducted toward the goals of crystallizing truncated EsaR proteins (Appendix A), solubilizing full-length EsaR (Appendix B) and establishing a β-galactosidase repression assay (Appendix C). For all work presented in the appendix, *Escherichia coli* Top10 cells were grown, stored and transformed as stated in the Materials and methods section of Chapter Two. The plasmids and *E. coli* strain used in these experiments are described in Table A.1.

Table A.1. Utilized plasmids and strains.

Plasmid/Strain	Relevant Information	Reference(s)
pHMGE	*attb*-His_6-MBP-TEV-Gly_5- *esaR-attb* under P_{tac}, Amp^r, derived from pDEST-HisMBP	(1)
pHMGNTD178	pHMGE encoding only for EsaR 1-178, Amp^r	(1)
pHMGNTD169	pHMGE encoding only for EsaR 1-169, Amp^r	(5)
pSUP102-*esaR*	*esaR* under $P_{BAD,}$ Cm^r	(6)
pMAL-P2	Backbone of pDEST-periHisMBP, *malE* under P_{tac}, Amp^r	(7, 8)
pSUP102	Compatible with pMAL-P2 vectors, Cm^r	(9)
pRNP-*lacZ*	natural promoter region of *esaR* fused to *lacZ*, Km^r, derived from pEXT22	(6)
***E. coli* Top10**	Commercially available from Life Technologies	(2)

Appendix A

Purification of truncated HMGE proteins

X-ray crystallography of EsaR would be a direct method of determining the protein structure. The full-length protein is difficult to purify in a soluble and concentrated form, so more soluble truncated EsaR proteins were developed by J. Koziski and J. Geissinger (5, 10). J. Koziski truncated the *esaR* gene. J. Geissinger created the pHMGNTD178 and pHMGNTD169 plasmids. Below is a description of the purification process. It follows the method established by J. Geissinger with the two exceptions of using sonication to lyse cells and using "salty" Ni binding buffer (750 mM NaCl, 20 mM HEPES, 20 mM imidazole, 10% glycerol, pH 7.4) (5).

Truncated EsaR proteins NTD178 (to residue 178) and NTD169 (to residue 169) were each purified by nickel affinity purification from 6 L of cell culture as described in Chapter Two, "Heterodimerization assay – coincubation method" using a 30 ml Ni-NTA column provided by the lab of F. Schubot (Virginia Tech). Harvested cells were resuspended in at most 60 ml and lysed using a Branson sonifier 450 (settings: timer = hold, duty cycle = 70%, output control = 8, sonicated for 30s and rested for 30s, repeated 5 to 10 times). Cell debris and aggregates were removed by two rounds of centrifugation (once at 10,000 rcf in a Beckman Coulter JA-25.50 rotor for 30 min at 4°C and a second time at 164,000 rcf in a Beckman Coulter Type 70 Ti rotor for 60 min at 4°C) and by passing the lysate through a 0.22 μm pore-size filter (bottle top vacuum filter with a polyethersulfone membrane, Corning). The salty Ni binding buffer contained 750 mM NaCl instead of 500 mM to further discourage protein contaminant interaction with the desired protein or the column.

Eluted fractions containing HMGNTD178 or HMGNTD169 (His-MBP tagged NTD178 and NTD169) were pooled and dialyzed against excess salty Ni binding buffer overnight at 4°C. The protein was concurrently subjected to proteolysis by His-tagged tobacco etch virus protease (variant S219V (11), kindly provided by the Schubot Lab) in a ratio of 1:100 of protease to HMGNTD178 or HMGNTD169 by mass. The resulting dialyzed and cut NTD178 or NTD169 protein was passed over a 40 ml Ni-NTA column (from the lab of F. Schubot) to remove the His-MBP tag and the protease. Gel filtration was performed as a final purification step in a HiPrep 26/60 Sephacryl S-200 HR column (GE Healthcare). NTD178 or NTD169 was eluted in HMGE working buffer (500 mM NaCl, 20 mM HEPES, 10% glycerol, pH 7.4) and was concentrated to 1 – 3 mg/ml by filtrating out excess buffer using a 44.5 mm (10 kD) ultrafiltration disc (Millipore) before giving it to the lab of F. Schubot (Virginia Tech) for crystallization studies.

Appendix B

Previous work in the lab of A. Stevens has found that it is difficult to cleave off the His-MBP tag from HMGE using TEV and to keep the resulting EsaR protein soluble (5). The wild-type protein can be purified without the tags, but that process is also difficult to reproduce (1).

TEV cleavage and solubilization of HMGE using arginine and glutamate

The solubility of proteins can sometimes be increased by including the amino acids L-arginine and L-glutamate in the buffer (12) (S. Melville, personal communication). A trial experiment with HMGE was attempted as described below.

HMGE was purified from 1 L of cell culture using a 5 ml HisTrap column. A step elution of 5 ml each of 15%, 30% and 50% Ni elution buffer was used instead of a gradient elution. Protein in the elutant containing 30% Ni elution buffer (500 mM NaCl, 20 mM HEPES, 300 mM imidazole, 10% glycerol, pH 7.4) was diluted to 0.5 mg/ml with salty Ni binding buffer. In a 15 ml conical tube, 1 ml HMGE was mixed with 0.1 ml TEV (1 mg/ml) and/or 0.2 ml of a 300 mM L-arginine and 300 mM L-glutamate mixture. Samples were brought to 1.3 ml with salty Ni binding buffer. The tubes were left overnight at 4°C, gently shaking. The following morning, 500 ml of each sample was pipetted into an Eppendorf tube which was then centrifuged at 20,000 rcf for 20 min at 4°C to pellet any suspended aggregates or precipitates. Samples from the centrifuged and not centrifuged portions were prepared for SDS-PAGE analysis as described in Chapter Two. Absorbance measurements at 280 nm were taken to determine if there was a loss of solubilized protein after centrifugation. This work was not duplicated.

There were visible differences among the samples when analyzed by SDS-PAGE (Fig. A.1). The HMGE protein seemed to be more readily cleaved by TEV when not in the presence of the amino acids. In Fig. A.1, in comparing lanes T-B/A (no added amino acids) to lanes TER-B/A (with added amino acids), the full-length HMGE protein (73 kD) is virtually absent in the T-B/A lanes. However, the same sample (T-B/A) also experienced the greatest loss of soluble protein (Table A.2). Samples with the amino acids did not lose any soluble protein.

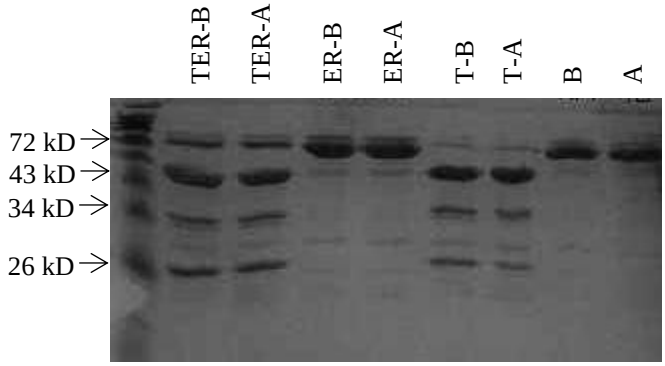

Figure A.1. TEV cleavage efficiency of HMGE in the absence and presence of arginine (R) and glutamate (E). A Coomassie-stained 12% SDS-PAGE gel is shown. Lanes are labeled to indicate which samples included TEV (T) and/or the amino acids (ER). Samples before (B) and after (A) centrifugation were loaded. Samples without TEV or the amino acids are simply labeled B and A. The predicted sizes of HMGE monomer, MBP, TEV and EsaR are 73 kD, 45 kD, 29kD and 28 kD, respectively.

Table A. 2. Retention of soluble protein after TEV cleavage of HMGE.[a]

Sample	A_{280}	Percent change (%)
TER-B	0.075	0
TER-A	0.075	
ER-B	0.062	+3.2
ER-A	0.064	
T-B	0.061	-20
T-A	0.049	
B	0.042	-14
A	0.036	

[a]Sample labeling follows that used in Fig. A.1.

TEV cleavage and solubilization of HMGE using DNA

Purification of EsaR in the presence of its target DNA sequence may help solubilize the protein. If there is a conformational shift upon binding to DNA, then the TEV recognition sequence might become more or less exposed. To test this, HMGE was purified as described in the previous section. DNA was prepared by as described in Chapter Three, "FRET assays, heterodimerization binding curves and distance calculations". In an Eppendorf tube, 500 µl HMGE was mixed with 50 µl TEV (0.3 mg/ml) and/or 100 µl of 25 µM DNA. Samples were brought to 650 µl with regular Ni binding buffer (500 mM NaCl, 20 mM HEPES, 20 mM imidazole, 10% glycerol, pH 7.4). The tubes were left overnight at 4°C. Samples were prepared for SDS-PAGE analysis as described in Chapter Two. Five microliters of each sample was loaded into a well of a 12% SDS-PAGE gel.

Within these experiments, there were discernable but non-reproducible differences in the efficiency of cleavage by TEV (Fig. A.2). This inconsistency reflected the difficulty of reproducing TEV cleavage of HMGE (A. Stevens and R. Ramachandran, personal communication). If this work is repeated in the future, then centrifugation should also be employed as done in the previous section to determine if the proteins are able to remain soluble.

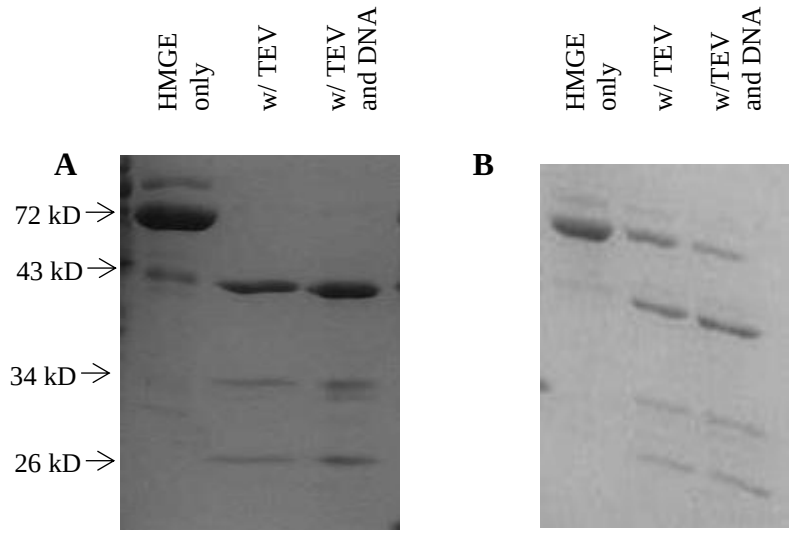

Figure A.2. TEV cleavage efficiency of HMGE in the absence and presence of DNA. A Coomassie-stained 12% SDS-PAGE gel is shown. Lanes are labeled indicate which samples included TEV and/or DNA. The predicted sizes of HMGE monomer, MBP, and TEV and EsaR are 73 kD, 45 kD, 34 kD and 28 kD, respectively. The results from repeated experiments are shown.

Appendix C

β-galactosidase repression assay

This work was performed by former undergraduate student Chris Brassell. A β-galactosidase (β-gal) repression assay was carried out using the Tropix Galacton-Star chemiluminescent assay kit. The manufacturer's directions were followed. *E. coli* Top 10 cells were cotransformed with three plasmids (pRNP-*lacZ*, pSUP102-*esaR*, pHMGNTD169/178 or the corresponding backbone vectors) (Table A.1, Fig. A.3). Cultures were grown overnight in LB medium supplemented with ampillicin (100 μg/ml), chloramphenicol (20 μg/ml) and kanamycin (50 μg/ml). The following day, subcultures were performed to an OD_{600} = 0.05. HMGE and EsaR overexpression was induced with the addition of IPTG (to 1 mM) and L-arabinose (to 0.02%). The cultures were allowed to grow at 30°C until the OD_{600} increased to 0.5. The cultures were diluted to the same turbidity (OD_{600} = 0.5) before collecting sample aliquots and storing them at -70°C. Measurements of β-gal activity were conducted with a Beckman Coulter LD 400S Luminescence Detector.

It was hypothesized that coexpression of the truncated HMGE proteins with EsaR would result in an increase of β-gal activity compared to a control in which only the wild-type protein was present. The truncated proteins lacked the C-terminal domain (CTD), which is required for binding to DNA (13, 14). HMGNTD178 was previously found to be able to dimerize (1). Heterodimer formation between EsaR and HMGNTD178 or HMGNTD169 would result in the EsaR not being able to bind to DNA and repress transcription of the β-gal gene. In the formed heterodimer, only one CTD would be present, which would not be enough for binding to the promoter region.

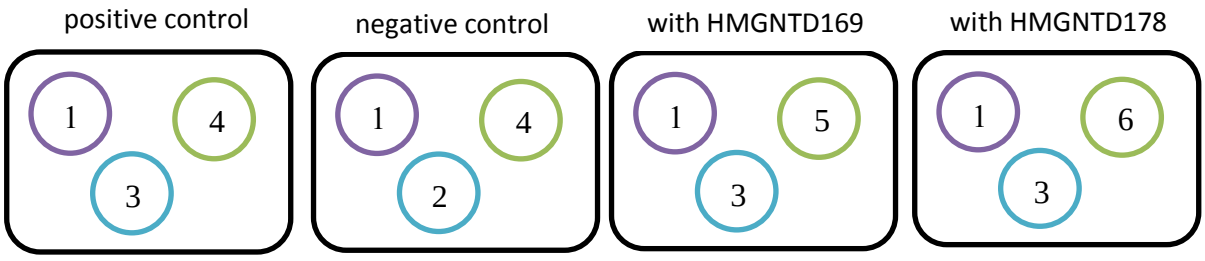

Figure A.3. Strain construction for β-galactosidase repression assay. Each cell type contained a set of three complementary plasmids: (1) pRNP-*lacZ*, (2) pSUP102, (3) pSUP102-*esaR*, (4) pMAL-P2, (5) pHMGNTD169, and/or (6) pHMGNTD178. The positive control was expected to have the least amount of β-gal activity as EsaR would repress expression of *lacZ*. The negative control would have the highest amount of β-gal transcription because the EsaR would not be present.

Results for the β-gal repression assay were as predicted (Fig. A.4). The positive control (cells with EsaR and without an HMGE variant) had the lowest amount of β-gal activity; the negative control (cells without EsaR or a HMGE variant), the most. The relative β-gal activities between the negative control and the sample EsaR and HMGNTD169 (without the linker region) could not be statistically distinguished (Table A.3). HMGNTD169 strongly interfered with repression of β-gal expression by EsaR. The presence of the linker region in HMGNTD178 may slightly hinder dimerization as β-gal expression was intermediate between the controls.

This work can be further developed into a high-throughput screen for identifying residues which are involved in dimerization. Potentially, randomly mutagenized pHMGNTD169 would be cotransformed with pRNP-*lacZ* and pSUP102-*esaR* into *E. coli*. Inability to suppress EsaR repression of β-gal expression would indicate the presence of a HMGNTD169 variant that is unable to dimerize with EsaR or is unstable.

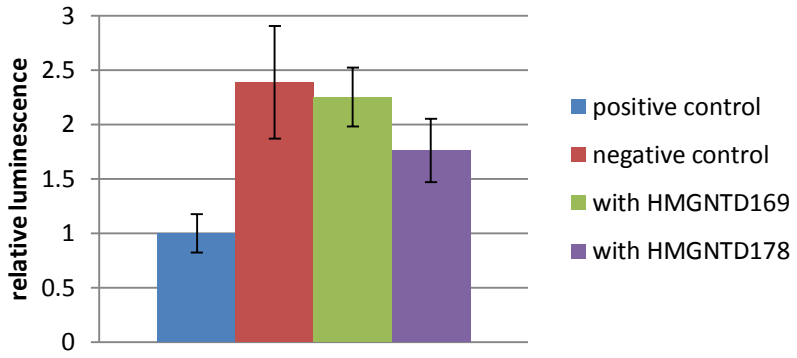

Figure A.4. β-galactosidase repression and derepression by EsaR and HMGE proteins. Samples were from the strains described in Figure A. 3. The data was normalized by averaging all replicates and dividing the averages by that of the positive control. In doing so, the positive control was set to a value of 1; the other samples were compared to it. Error bars represent one standard deviation above and below the mean.

Table A.3. Statistical comparisons of β-galactosidase repression assay results.

Sample	Relative Luminescence	Standard deviation	*p*-value (compared to pos. control)	*p*-value (compared to neg. control)	*p*-value (compared to w/HMGNTD169)
positive control	1	0.18			
negative control	2.39	0.52	3.69×10^{-4}		
w/HMGNTD169	2.25	0.27	3.99×10^{-6}	0.29	
w/HMGNTD178	1.76	0.29	2.65×10^{-4}	1.64×10^{-2}	6.48×10^{-3}

[a]The experiment was duplicated with triplicate sample analysis. Using Microsoft Excel, one-tailed heteroscedastic *t*-tests were performed to compare the average relative luminescence values. The significance level was set at 0.05.

References

1. Schu DJ, Ramachandran R, Geissinger JS, Stevens AM. 2011. Probing the impact of ligand binding on the acyl-homoserine lactone-hindered transcription factor EsaR of *Pantoea stewartii* subsp. *stewartii*. *J Bacteriol* 193:6315-22.
2. Zhang RG, Pappas KM, Brace JL, Miller PC, Oulmassov T, Molyneaux JM, Anderson JC, Bashkin JK, Winans SC, Joachimiak A. 2002. Structure of a bacterial quorum-sensing transcription factor complexed with pheromone and DNA. *Nature* 417:971-4.
3. Lintz MJ, Oinuma K, Wysoczynski CL, Greenberg EP, Churchill ME. 2011. Crystal structure of QscR, a *Pseudomonas aeruginosa* quorum sensing signal receptor. *Proc Natl Acad Sci U S A* 108:15763-8.
4. Chen G, Swem LR, Swem DL, Stauff DL, O'Loughlin CT, Jeffrey PD, Bassler BL, Hughson FM. 2011. A strategy for antagonizing quorum sensing. *Mol Cell* 42:199-209.
5. Geissinger JS. 2011. Structure-function analysis of the EsaR N-terminal domain. Master Thesis. Virginia Tech, Blacksburg.,
6. Schu DJ, Carlier AL, Jamison KP, von Bodman S, Stevens AM. 2009. Structure/function analysis of the *Pantoea stewartii* quorum-sensing regulator EsaR as an activator of transcription. *J Bacteriol* 191:7402-9.
7. Riggs P. 2000. Expression and purification of recombinant proteins by fusion to maltose-binding protein. *Mol Biotechnol* 15:51-63.
8. Nallamsetty S, Austin BP, Penrose KJ, Waugh DS. 2005. Gateway vectors for the production of combinatorially-tagged His6-MBP fusion proteins in the cytoplasm and periplasm of *Escherichia coli*. *Protein Sci* 14:2964-71.
9. Simon R, O'Connell M, Labes M, Puhler A. 1986. Plasmid vectors for the genetic analysis and manipulation of rhizobia and other Gram-negative bacteria. *Methods Enzymol* 118:640-59.
10. Koziski JM. 2008. Genetic analysis of the quorum sensing regulator EsaR. Biological Sciences, Master of Science.
11. Kapust RB, Tozser J, Fox JD, Anderson DE, Cherry S, Copeland TD, Waugh DS. 2001. Tobacco etch virus protease: mechanism of autolysis and rational design of stable mutants with wild-type catalytic proficiency. *Protein Eng* 14:993-1000.
12. Hautbergue GM GAP. 2008. Increasing the sensitivity of cryoprobe protein NMR experiments by using the sole low-conductivity arginine glutamate salt. *J Magn Reson* 191:335-339.
13. Stevens AM, Queneau Y, Soulere L, von Bodman S, Doutheau A. 2011. Mechanisms and synthetic modulators of AHL-dependent gene regulation. *Chem Rev* 111:4-27.
14. Fuqua WC, Winans SC, Greenberg EP. 1994. Quorum sensing in bacteria: the LuxR-LuxI family of cell density-responsive transcriptional regulators. *J Bacteriol* 176:269-75.